Scintillating Crystals for Dark Matter

The INFN School on Underground Physics

Riccardo Cerulli
INFN-Roma Tor Vergata
GSSI - June 22, 2022

OUTLINE

- Basic arguments on crystal scintillators (scintillation processes, light output, decay time, light collection, light readout)
- PMT: basic concepts, QE, low noise, low radioactivity features
- Light Guide and light collection
- Crystal scintillators for underground physics
- Example of rare processes successfully studied with crystal scintillators
- Crystal Scintillators for Dark Matter investigation
- Dark Matter Signatures for scintillators (diurnal, annual modulation, directionality)
- NaI(Tl) scintillators for Dark Matter: DAMA, ANAIS, KIM, SABRE, COSINE
- $ZnWO_4$; anisotropic scintillators, the directionality as a signature for Dark Matter with $ZnWO_4$
- New promising crystal scintillators for the future: CHC, CZC, SrI

Scintillators

- Scintillator:
  - a material that converts the kinetic energy of radiation passing throw into detectable light (scintillation light)
  - conversion must be efficient (good light yield)
  - the scintillation light has to «escape» from the material (no self absorption) and effectively collected
  - scintillation wavelength and decay time are important issues
  - the collected light is converted in electronic signal (light sensor at room temperature: PMT, APD, SiPM)
  - the material should have good optical properties, be easy to machine and to obtain in large size
  - material refractive index close to the glass one (1.5)

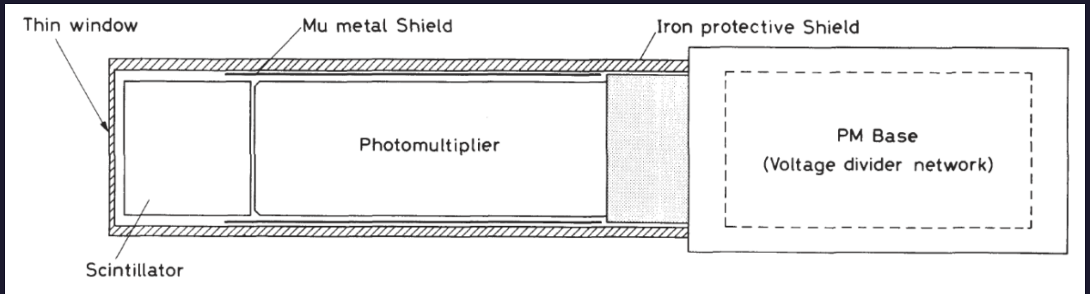

Scintillators

Classification:

- Organic scintillators:
  - aromatic hydrocarbon compounds containing benzene-ring structures; crystals, liquids, plastics;

    → see G. Ranucci talk
- Inorganic scintillators:
  - mainly alkali halides crystals containing a small activator impurity;
  - NaI(Tl), BGO, CsI(Tl), CaF_2, BaF_2, $CdWO_4$, $ZnWO_4$, SrI, $LaCl_3$, CHC, CZC, etc.

Scintillation Process

- Conduction band, valence band and forbidden band
- Presence in the forbidden band of activator centres due to the impurities added to the crystal; they produce "traps" for electron in the crystal lattice
- Energy released by radiation produces free e^-/hole going from valence to conduction band;
- Holes can ionize impurity atoms and free electrons can fall into this state and later decay to ground state emitting visible photons (energy < band gap)

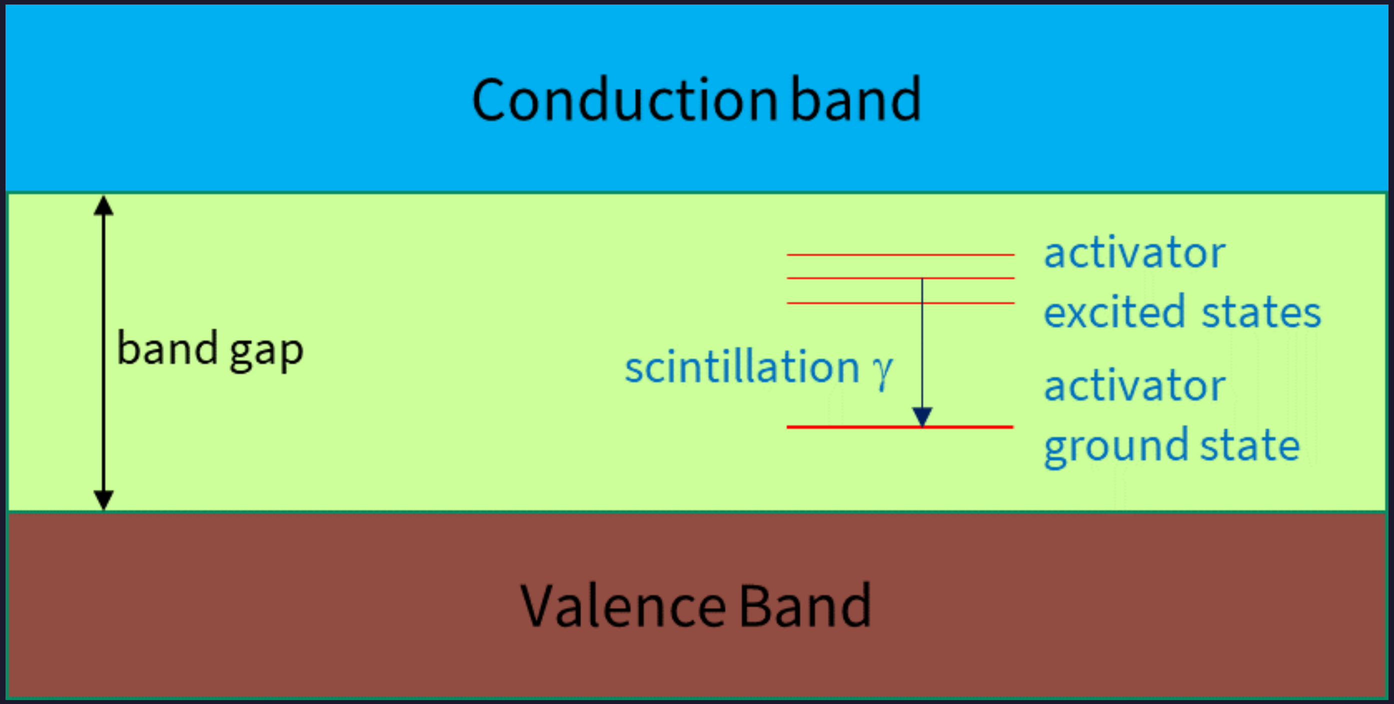

Scintillation Process

- Visible light is emitted with a characteristic efficiency that depends on the crystal and radiation (light output or light yield); process with non-visible photons production can occur
- Medium is generally transparent to the emitted light because the activator transition energy is smaller than the energy to produce e-/hole
- The light emitted by a scintillator has a characteristic spectrum

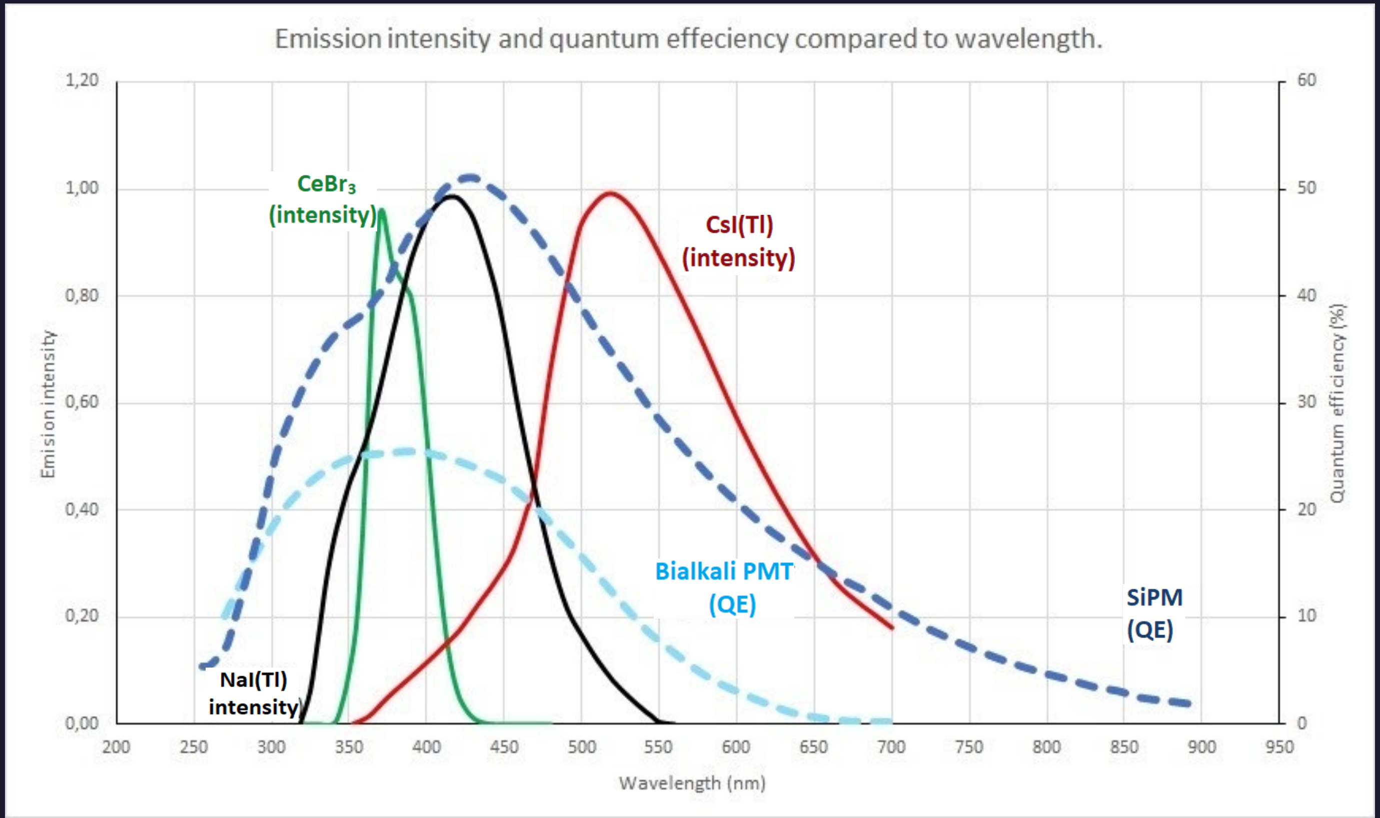

Light output and temperature dependence

- Birk's formula: light output per unit length

$$\frac{dL}{dx} = \frac{A\,\frac{dE}{dx}}{1 + kB\,\frac{dE}{dx}}$$

A – absolute scintillation efficiency;
kB – determined fitting data; for the same scintillator it depends on particles

- Proposed for organic can be used in some energy range also for inorganic crystals

- The non-linearity wrt Energy released per unit length is due to quenching interactions

- Light output in inorganic has a temperature dependence

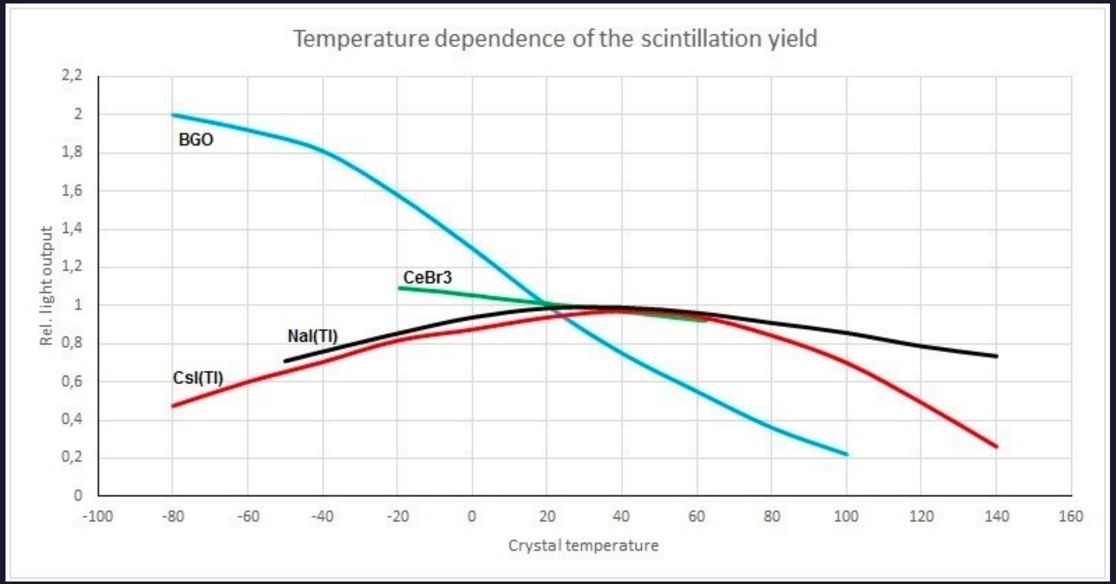

Scintillation decay time and Pulse Shape Discrimination

- Light emission can have more than one time decay component (fast, f; slow, s)
- Decay components depend on *dE/dX*
- Some scintillators have different decay components for different interacting particles ⇒ scintillation pulse shows different shape (PSD)

In alkali halides this depends on the density of free electrons and holes produced in the ionization process: high density (heavy particle) favours fast component

- Discrimination between γ/α and recoiling nuclei
- PSD very effective at MeV energy range

Time evolution of scintillation (*N* – number of emitted photons)

$$N = A \exp\left(\frac{-t}{\tau_f}\right) + B \exp\left(\frac{-t}{\tau_s}\right)$$

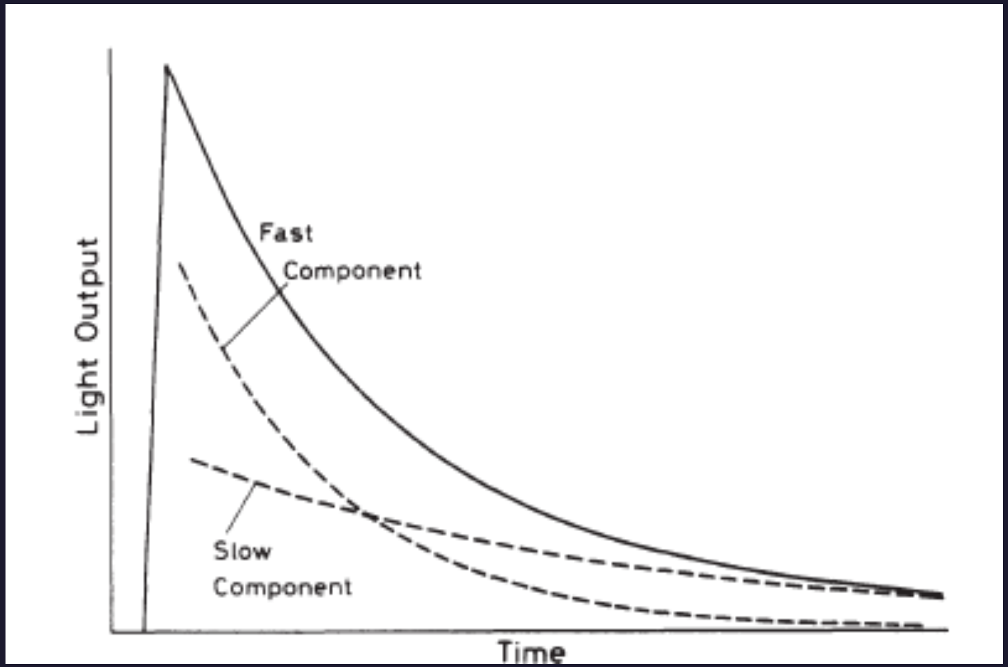

Properties of some Inorganic Scintillators

- Commonly used for spectroscopy
- Known since long time
- Various nuclei (high, low mass)
- Different time response

Table 8.3 Properties of Common Inorganic Scintillators

	Specific Gravity	Wavelength of Max. Emission	Refractive Index	Decay Time (μs)	Abs. Light Yield in Photons/MeV	Relative Pulse Height Using Bialk. PM tube	References
Alkali Halides							
NaI(Tl)	3.67	415	1.85	0.23	38 000	1.00	
CsI(Tl)	4.51	540	1.80	0.68 (64%), 3.34 (36%)	65 000	0.49	78, 90, 91
CsI(Na)	4.51	420	1.84	0.46, 4.18	39 000	1.10	92
Li(Eu)	4.08	470	1.96	1.4	11 000	0.23	
Other Slow Inorganics							
BGO	7.13	480	2.15	0.30	8200	0.13	
$CdWO_4$	7.90	470	2.3	1.1 (40%), 14.5 (60%)	15 000	0.4	98–100
ZnS(Ag) (polycrystalline)	4.09	450	2.36	0.2		1.3[a]	
CaF_2 (Eu)	3.19	435	1.47	0.9	24 000	0.5	
Unactivated Fast Inorganics							
BaF_2 (fast component)	4.89	220		0.0006	1400	na	107–109
BaF_2 (slow component)	4.89	310	1.56	0.63	9500	0.2	107–109
CsI (fast component)	4.51	305		0.002 (35%), 0.02 (65%)	2000	0.05	113–115
CsI (slow component)	4.51	450	1.80	multiple, up to several μs	varies	varies	114, 115
CeF_3	6.16	310, 340	1.68	0.005, 0.027	4400	0.04 to 0.05	76, 116, 117
Cerium-Activated Fast Inorganics							
GSO	6.71	440	1.85	0.056 (90%), 0.4 (10%)	9000	0.2	119–121
YAP	5.37	370	1.95	0.027	18 000	0.45	78, 125
YAG	4.56	550	1.82	0.088 (72%), 0.302 (28%)	17 000	0.5	78, 127
LSO	7.4	420	1.82	0.047	25 000	0.75	130, 131
LuAP	8.4	365	1.94	0.017	17 000	0.3	134, 136, 138
Glass Scintillators							
Ce activated Li glass[b]	2.64	400	1.59	0.05 to 0.1	3500	0.09	77, 145
Tb activated glass[b]	3.03	550	1.5	~3000 to 5000	~50 000	na	145
For comparison, a typical organic (plastic) scintillator:							
NE102A	1.03	423	1.58	0.002	10 000	0.25	

[a]for alpha particles

[b]Properties vary with exact formulation. Also see Table 15.1.

Source: Data primarily from Refs. 74 and 75, except where noted.

from «Radiation detection and measurement», G.F. Knoll

Light collection

- Largest possible fraction of scintillation light has to be collected
- Limiting factors: auto-absorption and loss at surface between crystal and encapsulating material, optical window, PMT (reflection)

$$\theta_c = \sin^{-1}\frac{n_1}{n_0}$$

critical angle for reflection;
n_0 – refraction index of scintillator

- If the light angle of incident is greater (smaller) than θ_c total (partial) internal reflection (and partial transmission) occurs; scintillators surrounded by a reflector
- Presence of light guide (transparent solid) from crystal to PMT limits light collection

Light readout

Scintillation light is collected and converted into electric signal:

- PMT, widely used (cost, dimension performances)
- APD made with semiconductor photodiodes, small surface, interesting for medical use (PET scanner)
- SiPm, arrays of APDs operating in Geiger Mode, low voltage, insensitive to magnetic field, compact but low gains, large noise at room temperature, cost/cm^2

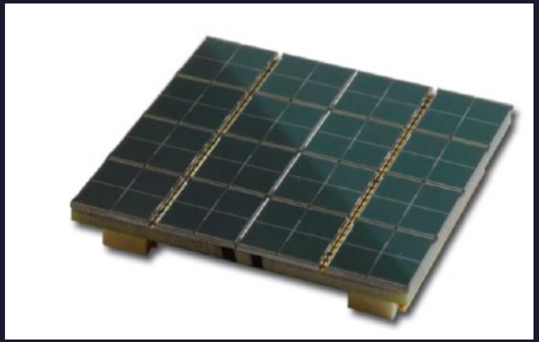

Photomultiplier Tube

- Photocathode made by photosensitive material converts scintillation photons into electrons; semiconductor material with alkali metals; multialkali material based on compound of Na_2KSb or K_2CsSb (bialkali)
- Electron collection system + an electron multiplier section (dynodes at different voltage)
- Anode collect electrons ⇒ signal
- All parts are inside a glass tube in vacuum

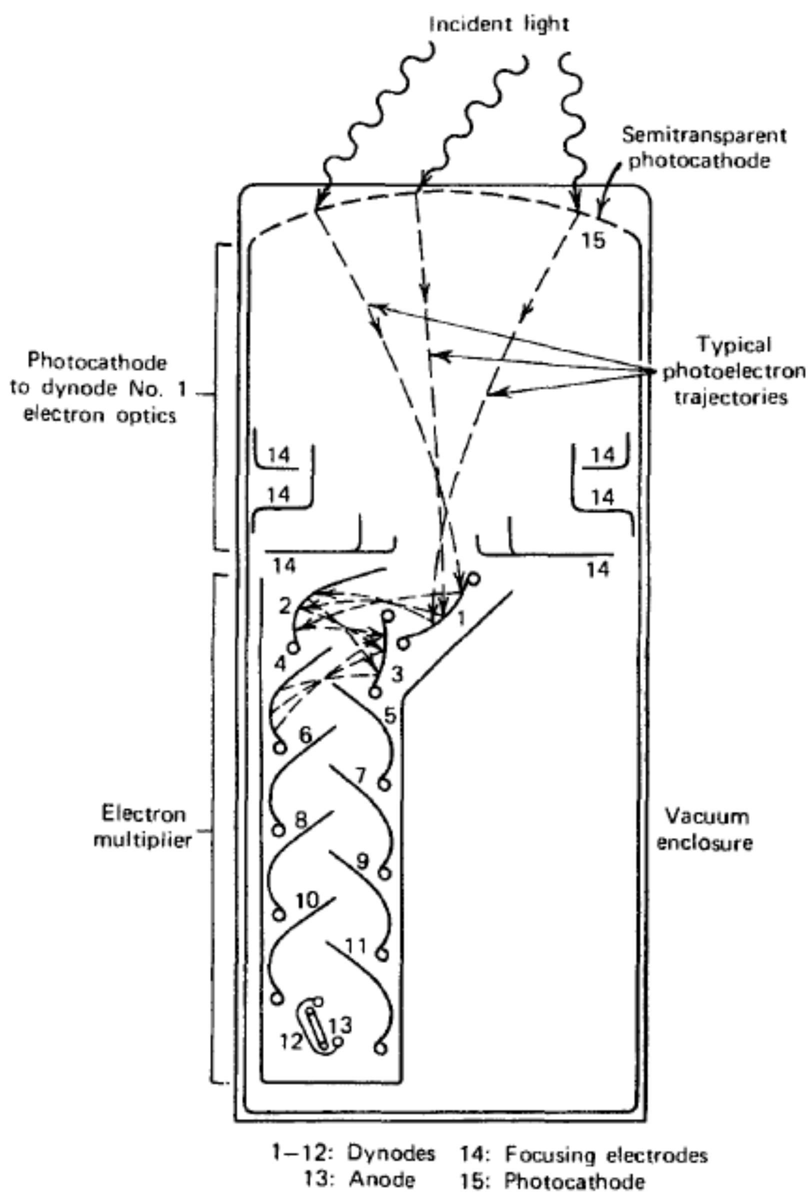

Figure 9.1 Basic elements of a PM tube. (From Ref. 1.)

from «Radiation detection and measurement», G.F. Knoll

Main characteristics of a PMT

- Quantum Efficiency (*QE*), sensitivity of photocathode:

$$QE(\lambda) = \frac{number\ of\ photoelectrons\ emitted}{number\ of\ incident\ photons\ (\lambda)}$$

QE depends on λ and it is typically 20-30%

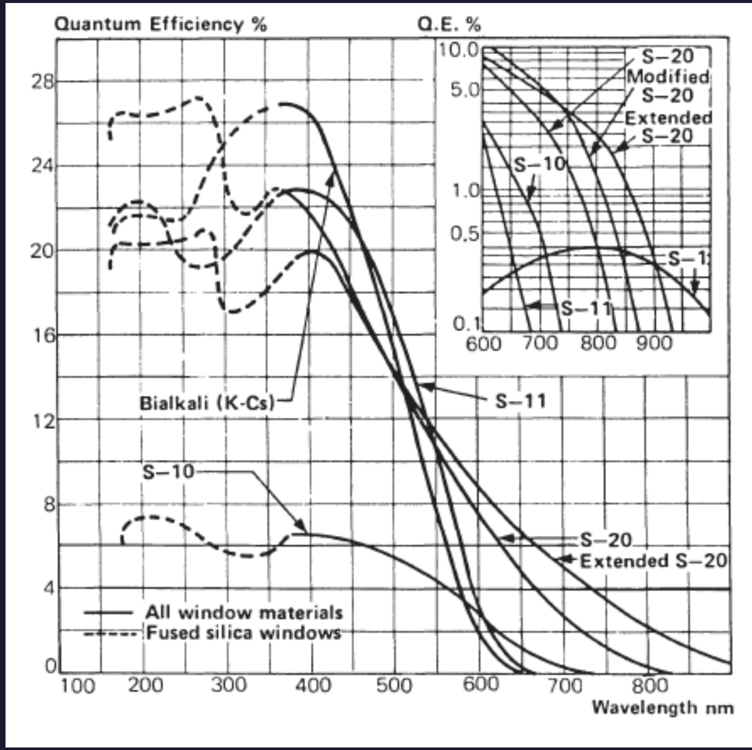

W.R. Leo, Techniques for Nuclear and Particle Physics Experiments

- Gain depends on secondary emission factor of dynodes (δ); it can arrive up to 10^7
- Noise and single ph. electron spectrum (peak/valley ratio)
- Dark current in cps
- Time response (rise time, transit time, transit time spread)

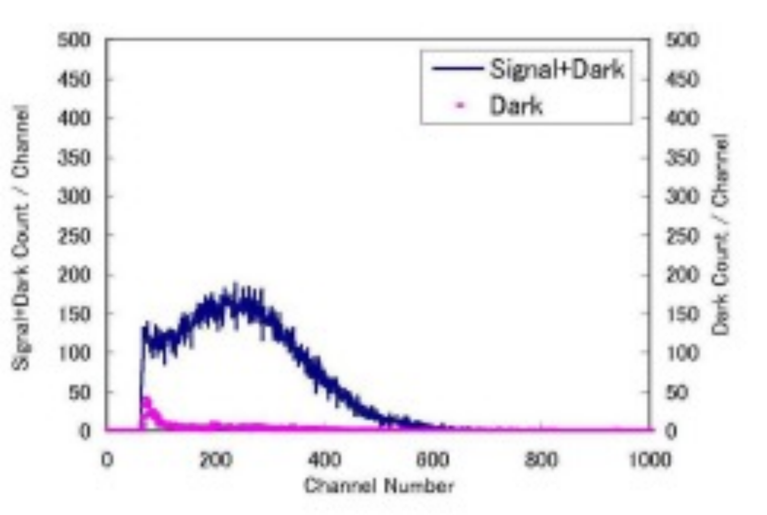

From Hamamatsu

Crystal Scintillators for underground physics

- various target materials (low and high mass nuclei)
- high detection efficiency for gamma/electrons
- compact
- chemical and mechanical stability
- high light yield ⇒ energy thresholds from keV
- stable with time
- good energy resolution
- control of the energy scale
- uniformity of the detector response
- PSD for gamma/alpha (recoil)

- high level of radiopurity to reach very low intrinsic background
- shielding by external environmental radiation (muons, neutrons, gammas, ...)

Crystal Scintillators for underground physics

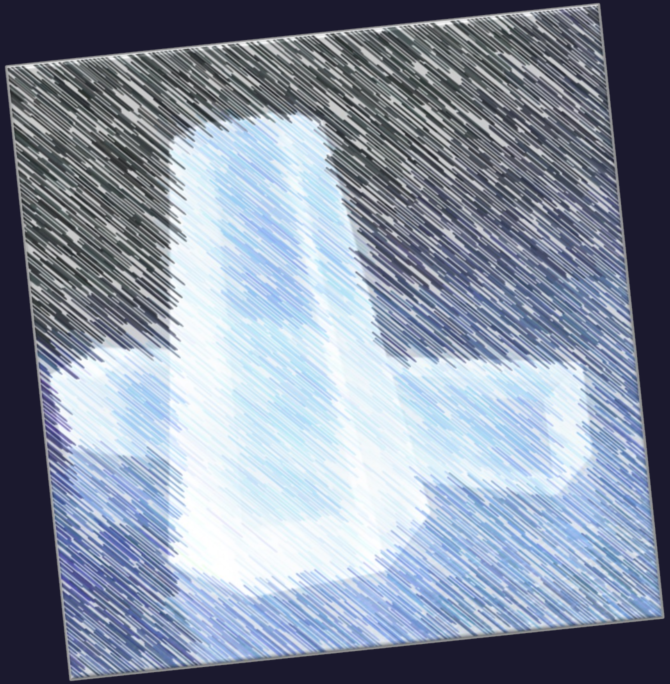

Inorganic scintillators have been successfully employed for rare processes search since the very beginning of the field:

- DM investigation (NaI(Tl), CaF_2, LXe, CsI(Tl))
- Double beta decay experiments (long list, see later)
- Solar axions (NaI(Tl), LiF, CsI(Tl))
- Exotic Matter search (NaI(Tl))
- Nuclear rare processes (rare α decay, cluster decay, superdense nuclear matter)

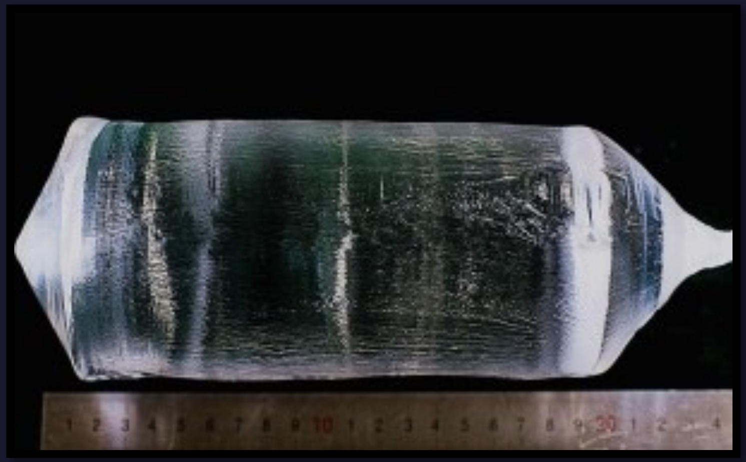

Developments of Inorganic scintillators with promising features still ongoing ($ZnWO_4$, SrI, CHC, CZN, etc.)

Intrinsic Radiopurity in Crystal Scintillator Detectors

- In inorganic scintillators presence of:
  - ^{232}Th, ^{238}U and ^{235}U families and ^{40}K,
  - cosmogenic and/or anthropogenic radionuclides
- Some scintillators contain elements with radioactive isotopes; e.g.:
  - ^{113}Cd in $CdWO_4$
  - ^{137}Cs in CsI(Tl)
  - ^{138}La in $LaCl_3$ and LaBr3

Achieving high radiopurity relies on a highly specialized experience and a long, delicate work (different phase, devoted measurements, many trials)

Intrinsic Radiopurity in Crystal Scintillator Detectors

- Procedures and protocols for the project/storage/cleaning/installation of the experiment, to reach high radio-purity level.
- Deep experience on the measurements and analysis techniques

- Pre-selection and analyses of materials (e.g. powders)
- Selection of growing processes
- Selection of additives
- Investigation on radioactive contaminants
- Chemical/physical purification of selected materials
- Growing protocols
- Identification of the optimal procedures and tools for crystal processing
- Selection of housing and materials in the surrounding environment
- Underground tests

positive outcome: improvement in radio-purity

production of detectors

See e.g. Instruments 2021, 5, 16; Physics 2021, 3, 187

Measurement techniques of radioactive contaminations

See e.g. Instruments 2021, 5, 16; Physics 2021, 3, 187

- ULB HP-Ge detectors, spectrometry: maximal sensitivity mBq/kg for U, Th, K; no sensitive to internal α contamination

- Atomic Absorption Spectrometer (AAS); wavelengths of light absorbed by the different elements are used to evaluate their concentrations in the solutions: good sensitivity (at ppb, sub-ppb level)

- Inductively Coupled Plasma Mass Spectroscopy (ICP-MS): mass-to-charge ratio (m/e) is used to identify the isotopes (no sensitive to short half-lives isotopes); peaks in the mass spectrum have an intensity proportional to the isotope concentration (^{232}Th up to : $\sim$ (0.8 – 0.008) mBq/kg, ^{238}U up to $\sim$ (2–0.02) mBq/kg; ^{40}K activity $\sim$ (0.3 – 6) mBq/kg)

→ final low background measurement can assure the highest sensitivity to the identification of the internal contaminants (high detection efficiency, for α and β particles)

Typical low background scintillation set-up

- Scintillators
- PMT: low background photomultiplier tubes; noise rejection at low energy (efficiencies)
- Light-guide to shield the scintillator from radioactivity of photomultiplier tubes (typically, the most contaminated materials of the set-up)
- Light guides made of a scintillation material with different (relative to the main scintillation detector) scintillation decay time can serve as active anticoincidence detectors
- Passive shield: layers of Lead, Copper, Neutron moderator (PE), Cadmium
- Set-up in Nitrogen atmosphere to suppress environmental Radon
- Active shield: shield counters surrounding the main detector, anti-muon veto counters;
- background suppression by using data on time of arrival and pulse-shape of scintillation signals

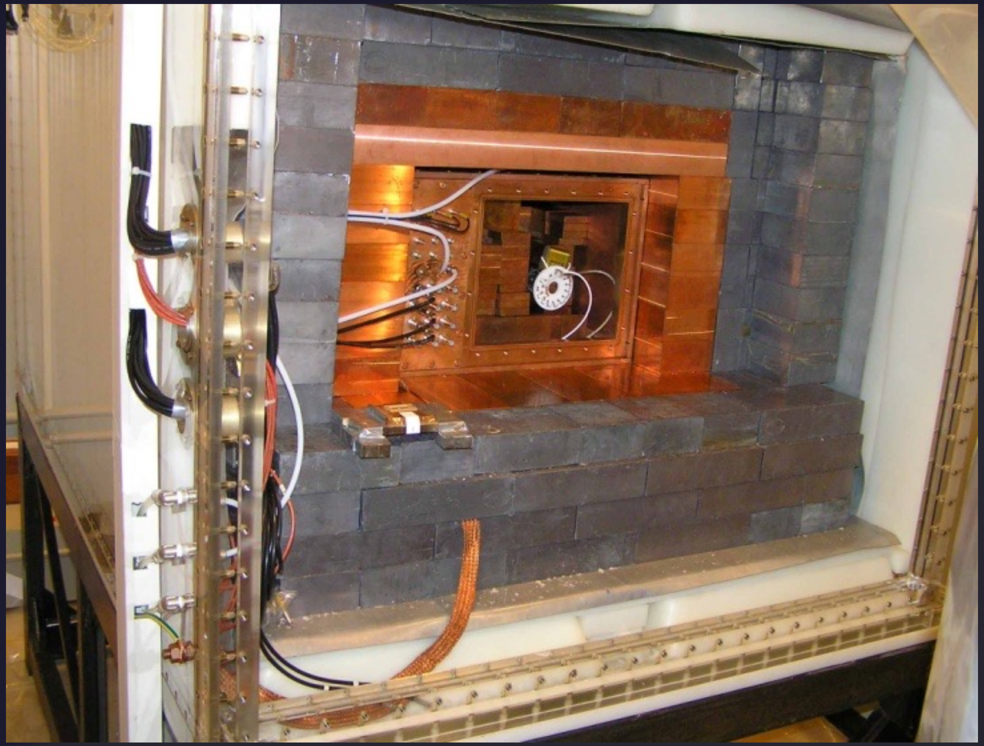

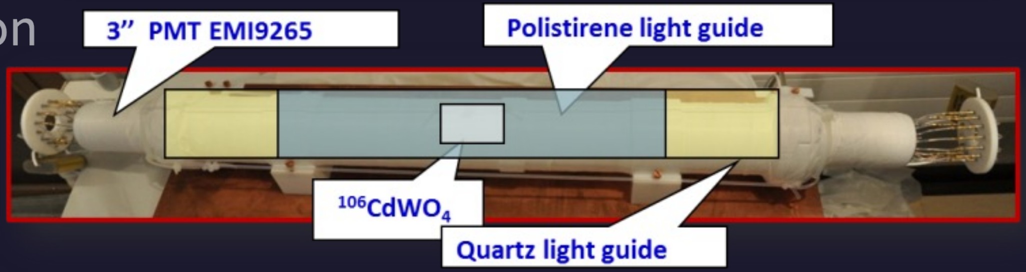

Intrinsic Radiopurity in Crystal Scintillator Detectors: a comparison for NaI(Tl)

Table 7. Radioactive contamination of NaI(Tl) crystal scintillators.

Chain	Source	Activity (mBq/kg) in sample, Reference							
		3.5 kg Ref. 224 UK DM	10.7 kg, Refs. 246 and 247 12.5 kg, Refs. 248–250 ANAIS	9.7 kg × 25 Ref. 209 DAMA/LIBRA	∅72 × 72 mm Refs. 251, 252 PICO-LON	3.4 – 9.6 kg Refs. 253–255 KIMS-NaI	8.47 kg Ref. 256 DM-Ice17	2 kg Ref. 257 SABRE	8 – 18 kg Ref. 258 COSINE-100
	^{3}H		0.2	< 0.09					
	^{22}Na			< 0.015					
	^{24}Na			< 0.00026					
	^{40}K		1.1 – 21	0.6	81(7)	0.8 – 1.5	17	0.3	0.5 – 2.5
	^{85}Kr			< 0.01					
	^{87}Rb			< 0.3				< 0.09	
	^{129}I		0.94	0.95(6)			1		
^{232}Th	^{232}Th		0.0007 – 0.004	0.0085(5)	0.002 – 0.24		0.01	< 0.004	< 0.001 – 0.01
	^{228}Ra						0.16		
	^{228}Th	0.014		0.002 – 0.03		0.0008 – 0.04	0.17 – 0.18		
	^{216}Po		0.02		0.013(8)				
^{238}U	^{238}U	< 0.005		0.0044(7)	< 0.0005 – 0.52		0.017	< 0.01	< 0.0002 – < 0.0015
	^{234}U		2.7 – 10	0.0158(16)			0.14		
	^{226}Ra	0.045	0.2	0.0217(11)	0.105(17)	< 0.0002– < 0.015	0.93 – 0.96		
	^{210}Pb		0.7 – 3.15	0.0242(16)	0.03 – 9.6		1.5		
	^{210}Po		0.6						
Total α activity			0.58 – 3.15	≈ 0.08		0.48 – 3.29			0.74 – 3.20

From IJMPA 33, No. 09, 1843007 (2018)

Intrinsic Radiopurity in Crystal Scintillator Detectors: a comparison

Table 13. Radioactive contamination of magnesium ($MgWO_4$), calcium ($CaWO_4$), zinc ($ZnWO_4$) and lead ($PbWO_4$) tungstate crystal scintillators.

Chain	Source	Activity (mBq/kg) in sample, Reference								
		$MgWO_4$	$CaWO_4$				$ZnWO_4$		$PbWO_4$	
		0.9 g Ref. 216	54 g Ref. 268	189 g Ref. 155	328 – 740 g Ref. 196	155 – 310 g Refs. 269, 270	163 g Ref. 192	117 – 699 g Ref. 156	182 g Ref. 271	454 g[b] Ref. 161
	^{40}K	$< 1.6 \times 10^3$	< 100	< 12	< 21	< 20	< 321	< 0.02		
	^{65}Zn							$0.5(1) - 0.8(2)$		
	$^{90}Sr-^{90}Y$	$< 1.5 \times 10^3$		< 70	< 26			< 0.1		
	^{137}Cs		< 10	< 0.8		< 1.2		< 0.05		
	^{147}Sm	< 540	$6(2)$	$0.49(4)$				< 0.01		$0.007(5)$
^{232}Th	^{232}Th	< 280	< 0.2	$0.69(10)$	< 9	$0.009(2)$		< 0.03		$0.051(8)$
	^{228}Ra					< 2.1, $0.015(4)$		< 0.02		
	^{228}Ac		< 40				< 125			
	^{228}Th	< 50	< 30	$0.6(2)$	< 6	< 1.6		$0.002(2) - 0.018(2)$	< 13	
	^{212}Pb		< 200				< 316			
	^{212}Bi		< 80				< 267			
^{235}U	^{235}U					$0.040(4)$	< 3610			
	^{227}Ac			$1.6(3)$		$0.098(20)$		$< 0.003 - 0.011(3)$		
	^{211}Pb						< 162			
^{238}U	^{238}U		$40(4)$	$14.0(5)$	$38(14) - 330(17)$	< 68, $1.01(2)$				< 0.01
	$^{238}U+^{234}U$							< 0.08		
	^{234m}Pa		< 400				< 560			
	^{234}U					$1.08(3)$				< 0.007
	^{230}Th					$0.056(5)$		< 0.07		$0.178(15)$
	^{226}Ra	< 50	$7(2)$	$5.6(5)$	$4(2) - 107(11)$	$< 2.2 - 58$, $0.04(1)$	$< 30 \times 10^3$	$0.002(1) - 0.025(6)$	< 10	$1.403(43)$
	^{214}Pb		< 100				< 115			
	^{214}Bi		< 80			$0.047(5)$	< 159			
	^{210}Pb	$< 2.4 \times 10^3$	$900(70)$	< 430	$< 190 - 4800(200)$				$(53 - 79) \times 10^3$	
	^{210}Po	$5.7(4) \times 10^3$	$780(20)$	$291(5)$	$26(9) - 1316(17)$	$0.018(4)$		< 0.01		$186(1)$
Total α activity			930[a]	400	$240(20) - 1400(30)$	$1.2 - 107$, $3.08(4)$		$0.18(3) - 2.3(2)$		

[a]Estimated from the spectra presented in Fig. 13 of Ref. 268.
[b]$PbWO_4$ crystal produced from archaeological lead.

From IJMPA 33, No. 09, 1843007 (2018)

External radioactive contamination

- Contamination of PMT: devoted PMT R&D (glass, metallic, etc.), development and selection

	^{226}Ra (mBq/PMT)	^{235}U (mBq/PMT)	^{238}U (mBq/PMT)	^{228}Ra (mBq/PMT)	^{228}Th (mBq/PMT)	^{232}Th (mBq/PMT)	^{40}K (mBq/PMT)
DAMA	65	7		18	12		81
ANAIS	67		180			22	115

- Lead: use of lead with low concentration of ^{210}Pb; low radioactivity lead present in the market (Plumbum, Boliden, etc.) with activity <few-150 Bq/kg; archeological lead (<few mBq/kg)

- Copper: OFHC copper, low level of contamination (<0.5 ppb for ^{238}U, <0.6 ppm for ^{232}Th, <0.06 ppm for ^{nat}K)

- Other material: need for dedicated measurements

2β decay experiment with crystal scintillators

- First neutrinoless double decay experiment to search for ^{48}Ca with crystal scintillator in 1966 (CaF_2(Eu)) [der Mateosian and Goldhaber]
- Big number of scintillation materials contain double β active isotopes (source=detector approach)
- Presently many experiments use crystal scintillators ⇒ very competitive results
- $2\beta^+$ decay can be investigated with anticoincidence technique with 511 keV gammas
- Also hybrid technique in combination with bolometric measurement (see P. Gorla lecture)

From IJMPA 33, No. 09, 1843007 (2018)

2β transition	Scintillator	Main results: half-life (channels)
^{40}Ca→^{40}Ar	$CaWO_4$	$\geq 9.9\times10^{21}$ yr ($2\nu2K$)
	$CaWO_4$	$\geq 1.4\times10^{22}$ yr ($0\nu2\varepsilon$)
^{46}Ca→^{46}Ti	CaF_2(Eu)	$\geq 1.0\times10^{17}$ yr ($0\nu2\beta^-$)
^{48}Ca→^{48}Ti	CaF_2(Eu)	$\geq 5.8\times10^{22}$ yr ($0\nu2\beta^-$)
^{70}Zn→^{70}Ge	$ZnWO_4$	$\geq 3.8\times10^{18}$ yr ($2\nu2\beta^-$)
	$ZnWO_4$	$\geq 3.2\times10^{19}$ yr ($0\nu2\beta^-$)
^{64}Zn→^{64}Ni	$ZnWO_4$	$\geq 1.1\times10^{19}$ yr ($2\nu2K$)
	$ZnWO_4$	$\geq 9.4\times10^{20}$ yr ($2\nu\varepsilon\beta^+$)
^{82}Se→^{82}Kr	$Zn^{82}Se$	$\geq 2.4\times10^{24}$ yr ($0\nu2\beta^-$)
^{100}Mo→^{100}Ru	$ZnMoO_4$	$=[7.15\pm0.37(\text{stat.})\pm0.66(\text{syst.})]\times10^{18}$ yr ($2\nu2\beta^-$)
	$Li_2{}^{100}MoO_4$	$=[6.90\pm0.15(\text{stat.})\pm0.37(\text{syst.})]\times10^{18}$ yr ($2\nu2\beta^-$)
	$Li_2{}^{100}MoO_4$	$\geq 7.0\times10^{22}$ yr ($0\nu2\beta^-$)
	$^{48depl}Ca^{100}MoO_4$	$\geq 4.0\times10^{21}$ yr ($0\nu2\beta^-$)
^{106}Cd→^{106}Pd	$^{106}CdWO_4$	$\geq 1.1\times10^{21}$ yr ($2\nu\varepsilon\beta^+$)
	$^{106}CdWO_4$	$\geq 2.2\times10^{21}$ yr ($0\nu\varepsilon\beta^+$)
^{108}Cd→^{108}Pd	$CdWO_4$	$\geq 1.1\times10^{18}$ yr ($2\nu2K$)
	$CdWO_4$	$\geq 1.0\times10^{18}$ yr ($0\nu2\varepsilon$)
^{114}Cd→^{114}Sn	$CdWO_4$	$\geq 1.3\times10^{18}$ yr ($2\nu2\beta^-$)
	$CdWO_4$	$\geq 1.1\times10^{21}$ yr ($0\nu2\beta^-$)
^{116}Cd→^{116}Sn	$^{116}CdWO_4$	$=[2.69\pm0.02(\text{stat.})\pm0.14(\text{syst.})]\times10^{19}$ yr ($2\nu2\beta^-$)
	$^{116}CdWO_4$	$\geq 2.4\times10^{23}$ yr ($0\nu2\beta^-$)
^{136}Xe→^{136}Ba	Xenon-loaded	$=[2.21\pm0.02(\text{stat.})\pm0.07(\text{syst.})]\times10^{21}$ yr ($2\nu2\beta^-$)
	liquid scintillator	$\geq 1.07\times10^{26}$ yr ($0\nu2\beta^-$)
^{130}Ba→^{130}Xe	BaF_2	$\geq 1.4\times10^{17}$ yr ($0\nu\varepsilon\beta^+$)
^{136}Ce→^{136}Ba	$CeCl_3$	$\geq 3.2\times10^{16}$ yr ($2\nu2K$)
^{160}Gd→^{160}Dy	Gd_2SiO_5(Ce)	$\geq 1.9\times10^{19}$ yr ($2\nu2\beta^-$)
	Gd_2SiO_5(Ce)	$\geq 1.3\times10^{21}$ yr ($0\nu2\beta^-$)
^{180}W→^{180}Hf	$CaWO_4$	$\geq 3.1\times10^{19}$ yr ($2\nu2K$)
	$CaWO_4$	$\geq 9.4\times10^{18}$ yr ($0\nu2\varepsilon$)
^{186}W→^{186}Os	$ZnWO_4$	$\geq 2.3\times10^{19}$ yr ($2\nu2\beta^-$)
	$^{116}CdWO_4$	$\geq 1.1\times10^{21}$ yr ($0\nu2\beta^-$)

$[2.630\pm0.011(\text{stat})^{+0.113}_{-0.123}(\text{sys})\times10^{19}\text{ yr}]$ ($2\nu2\beta^-$)

Example of $2\beta^-$ decay experiment with crystal scintillators: the case of ^{116}Cd

^{116}Cd is one of the best isotopes to search for $2\beta0\nu$ decay:

- $Q_{2\beta}$ = 2813.49(13) keV:
  - (a) > 2615 keV of ^{208}Tl;
  - (b) th. point of view: $\Gamma(2\beta2\nu) \sim Q_{2\beta}^{11}$, $\Gamma(2\beta0\nu) \sim Q_{2\beta}^{5}$
- favourable th. estimations of NMEs for $2\beta0\nu$
- quite high isotopic abundance δ = 7.512(54)% and availability of enrichment by centrifugation (cheap) in large amounts

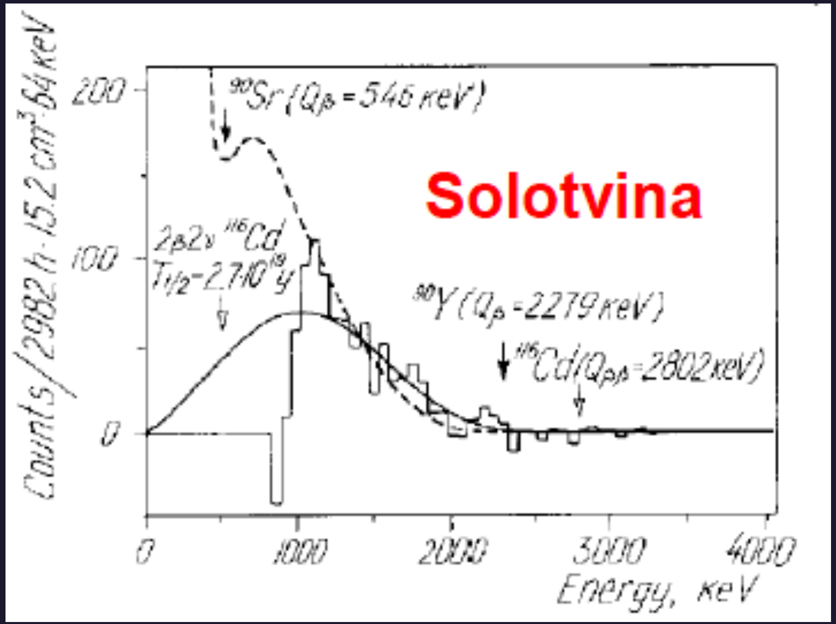

Positive Results for the $2\beta2\nu$ decay

Experiment	Technique	$T_{1/2}$ (10^{19} yr)	Year
ELEGANT V	^{116}Cd foils, drfit chambers, plastic scintillators	$2.6^{+0.9}_{-0.5}$	1995
Solotvina	$^{116}CdWO_4$ scintillators	$2.7^{+0.5}_{-0.4}$(stat) $^{+0.9}_{-0.6}$(sys)	1995
NEMO-2	^{116}Cd foils, track reconstruction by Geiger cells, plastic scintillators	3.75±0.35(stat)±0.21 (sys)	1995
Solotvina	$^{116}CdWO_4$ scintillators	2.6±0.1(stat) $^{+0.7}_{-0.4}$(sys)	2000
Solotvina	$^{116}CdWO_4$ scintillators	2.9±0.06(stat) $^{+0.4}_{-0.3}$(sys)	2003
NEMO-3	^{116}Cd foils, track reconstruction by Geiger cells, plastic scintillators	2.74±0.04(stat)±0.18 (sys)	2017
AURORA	$^{116}CdWO_4$ scintillators	2.630±0.011(stat)$^{+0.113}_{-0.123}$(sys)	2018

Most precise $T_{1/2}$ measurement obtained with scintillators

Phys.Rev.D 98, 092007 (2018)

Example of $2\beta^-$ decay experiment with crystal scintillators: the case of ^{116}Cd

Most precise measurement of $2\beta2\nu$ by AURORA Experiment at LNGS in DAMA/R&D set-up

- Two highly radiopure $CdWO_4$ enriched in ^{116}Cd at 82% (1.162 kg)
- liquid scintillator in anticoincidence
- low radioactive shield
- α/β PSD, TA analysis, Bi-Po events identification

$$T_{1/2}(2\beta2\nu) = (2.630 \pm 0.011(\text{stat})^{+0.113}_{-0.123}(\text{sys}))\times10^{19}\ \text{yr}$$

$$T_{1/2}(2\beta0\nu) > 2.2\times10^{23}\ \text{yr}$$

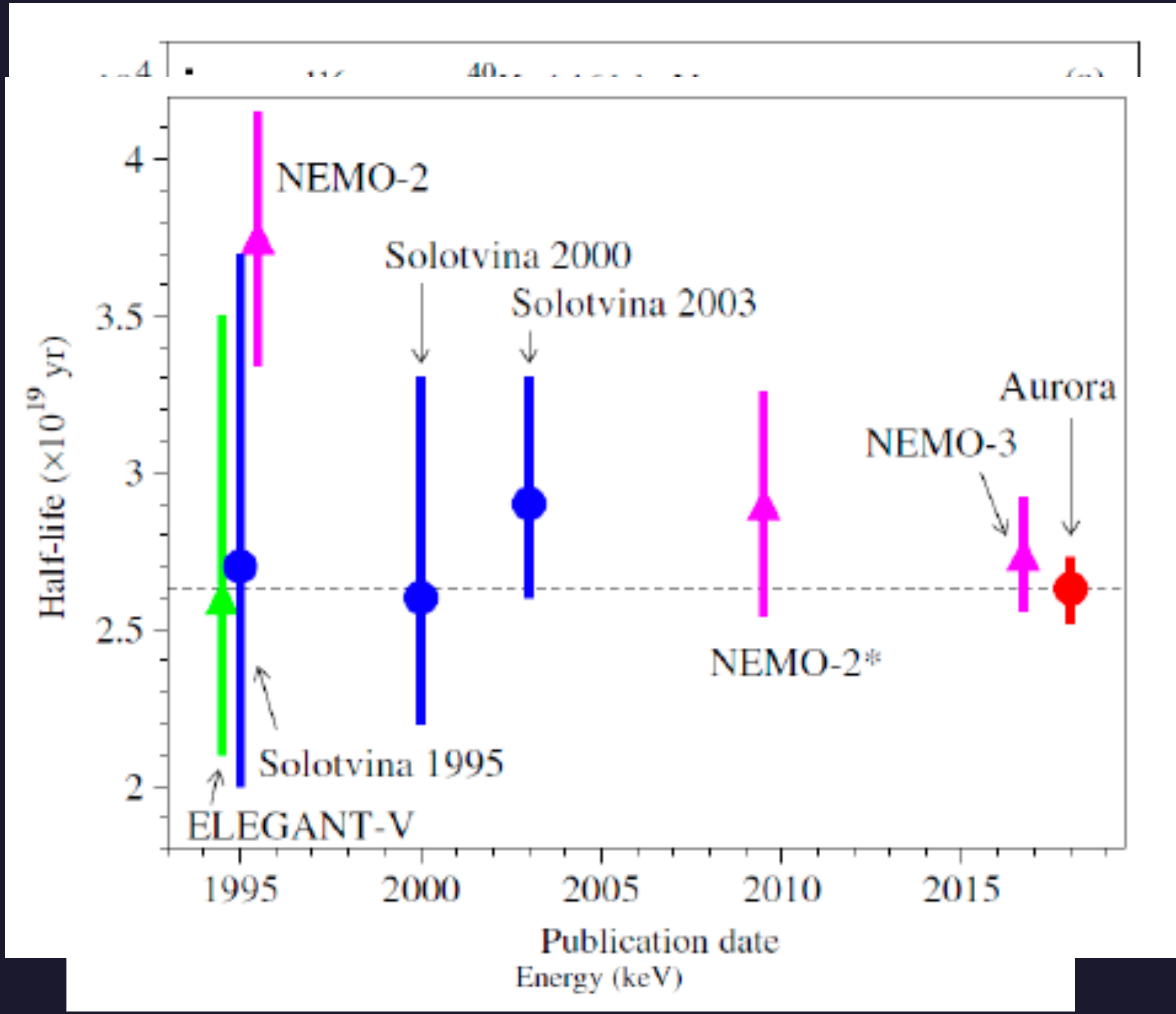

Phys.Rev.D 98, 092007 (2018)

Example of 2β⁺ decay experiment with crystal scintillators

- ^{130}Ba and ^{106}Cd 2β⁺ decay : coincidence of signal from the decay and subsequent gammas in adjacent detectors from e⁺ annihilation

- For ^{106}Cd 2β2ν decay $T_{1/2}$ limit at level od 10^{21}yr, in the region of theoretical expectation [experiment running, A. Leoncini et al. Phys. Scr. 97(2022)064006]

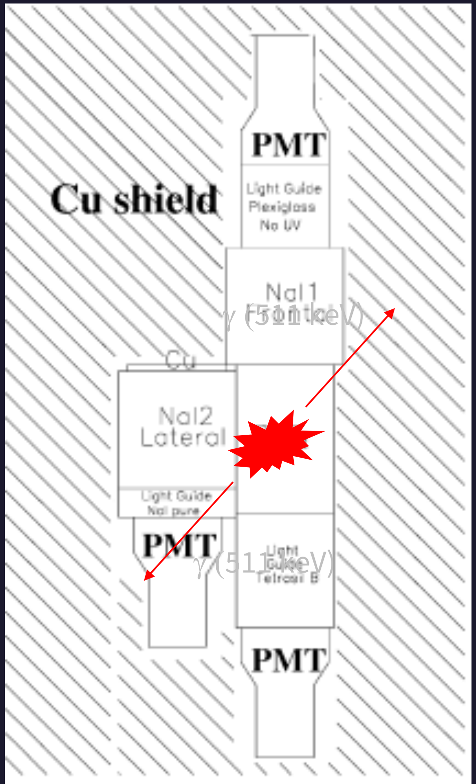

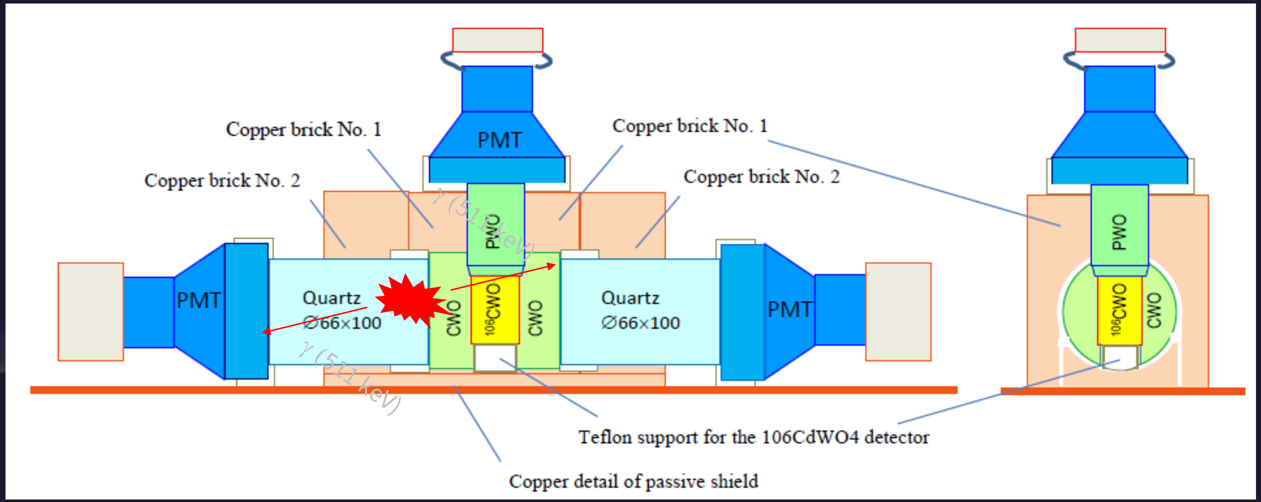

Rare processes search with crystal scintillators: the case of solar axion

<u>*Nature Physics*</u> **13**, 584–590 (2017)

- Solar Axion via Primakoff effect: coherent conversion of solar axions into photons in crystal lattice ($g_{a\gamma}$)
- Searched for e.g. in NaI(Tl) scintillator in DAMA [PLB515(2001)6]; still most sensitive results with Bragg technique
- Other results e.g. from Cosine-100 on g_{ae} [Astrop.Phys. 114 (2020)]

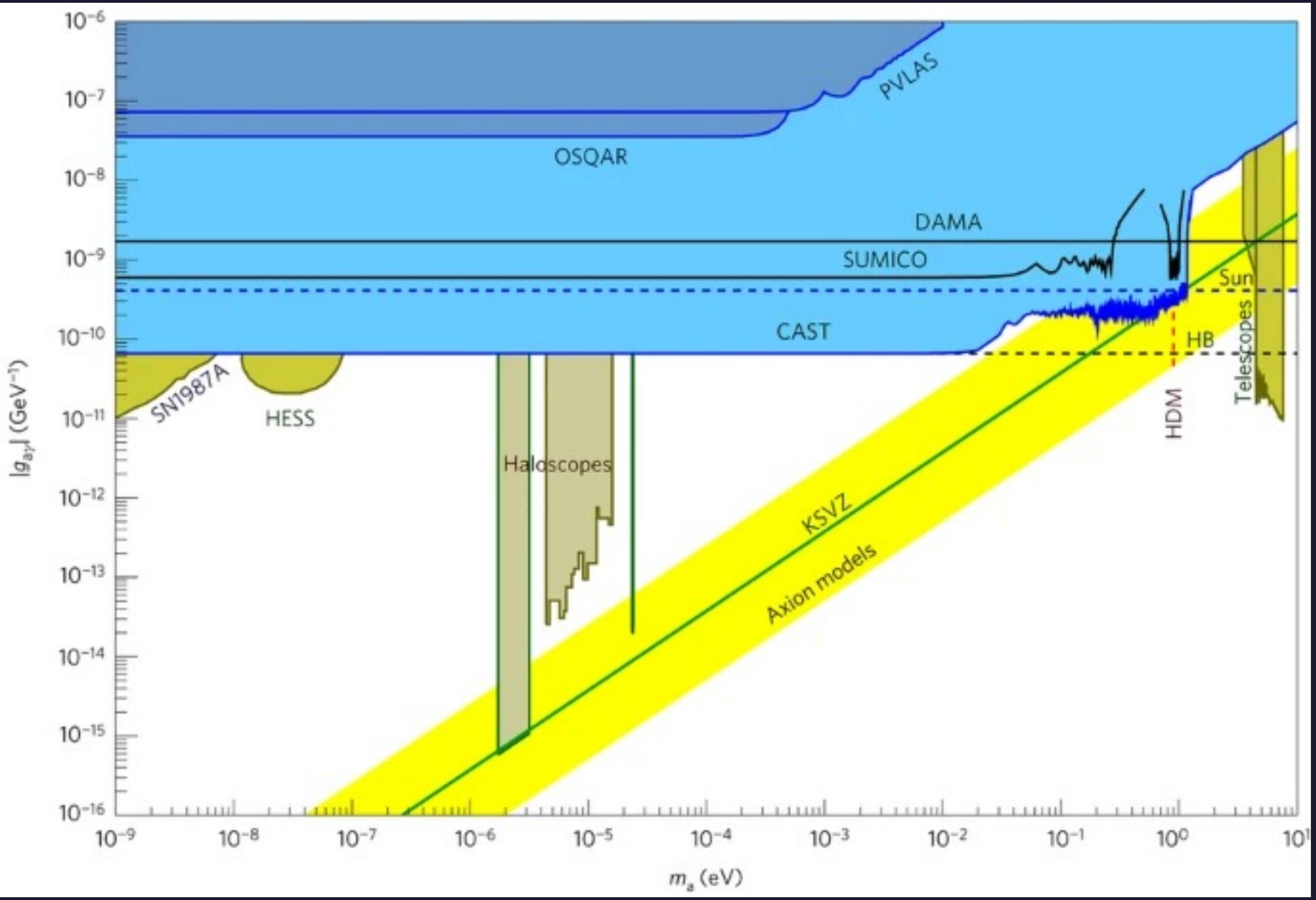

Dark Matter investigation with crystal scintillators

- Crystal scintillators have been exploited since the beginning for DM investigation
- Most important results have been obtained by DAMA/NaI and DAMA/LIBRA by employing Ultra-radiopure NaI(Tl)
- Other experiments in progress using NaI(Tl): ANAIS, COSINE (DM-ICE), SABRE, PICOLON
- Other interesting crystal scintillators considered:
  - CaF_2 (DAMA, Kamioka Observatory): SD coupling with Dark Matter particles
  - CsI(Tl) (KIMS)
- Promising crystal scintillators for future experiments:
  - $ZnWO_4$, SrI, ….

Dark Matter investigation with crystal scintillators: «traditional approach»

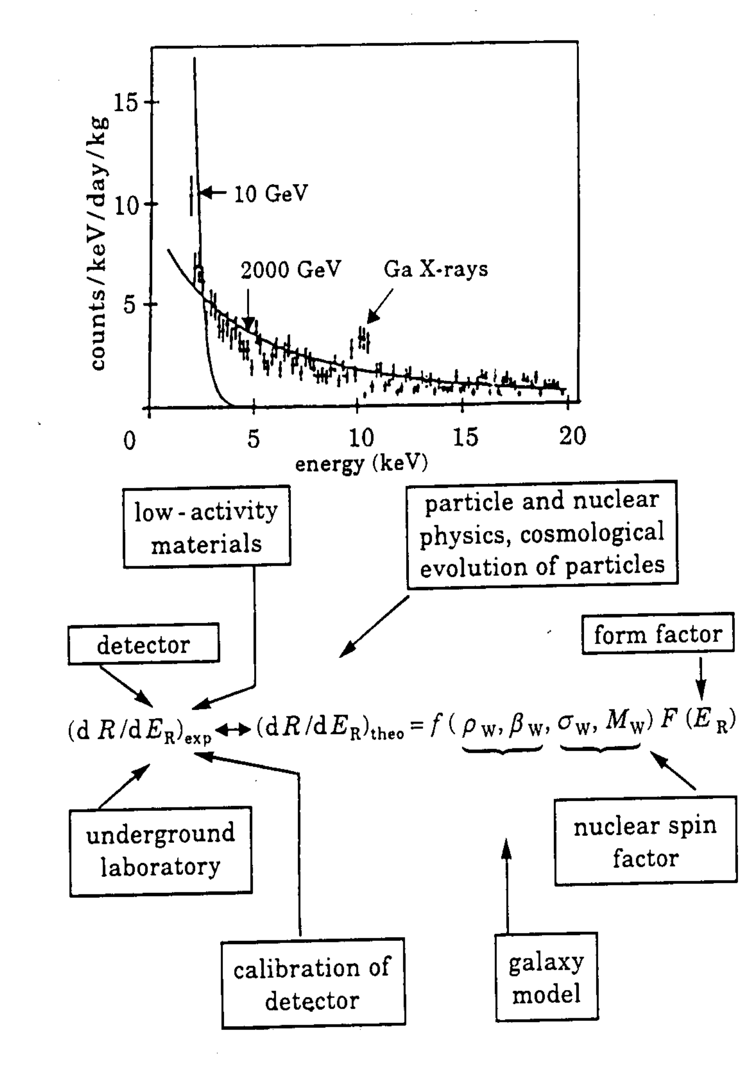

- Experimental vs Expected spectra (with or without e.m. component rejection)
- Several assumptions and modelling required ⇒ experimental and theoretical uncertainties generally not included in calculations
- Exclusion plot by fixing the model, all the assumptions and parameters

- No discovery potentiality
- Limitations in the recoil/background discrimination when applied
- Uncertainties in the exclusion plots and in comparisons (model dependent validity)

Dark Matter investigation with crystal scintillators: the nuclear quenching factor

- Quenching factor (q): ratio of the scintillation light measured for recoil and for electron of the same energy
- to be measured with neutron source or neutron generators
  - differences are often present in different experimental determinations of q for the same nuclei in the same kind of detector
  - e.g. in doped scintillators q depends on dopant and on the impurities/trace contaminants; in LXe e.g. on trace impurities, on initial UHV, on presence of degassing/releasing materials in the Xe, on thermodynamical conditions, on possibly applied electric field, etc.
  - Some time increases at low energy in scintillators (dL/dx)
  - … and more

Quenching factor for Na and I

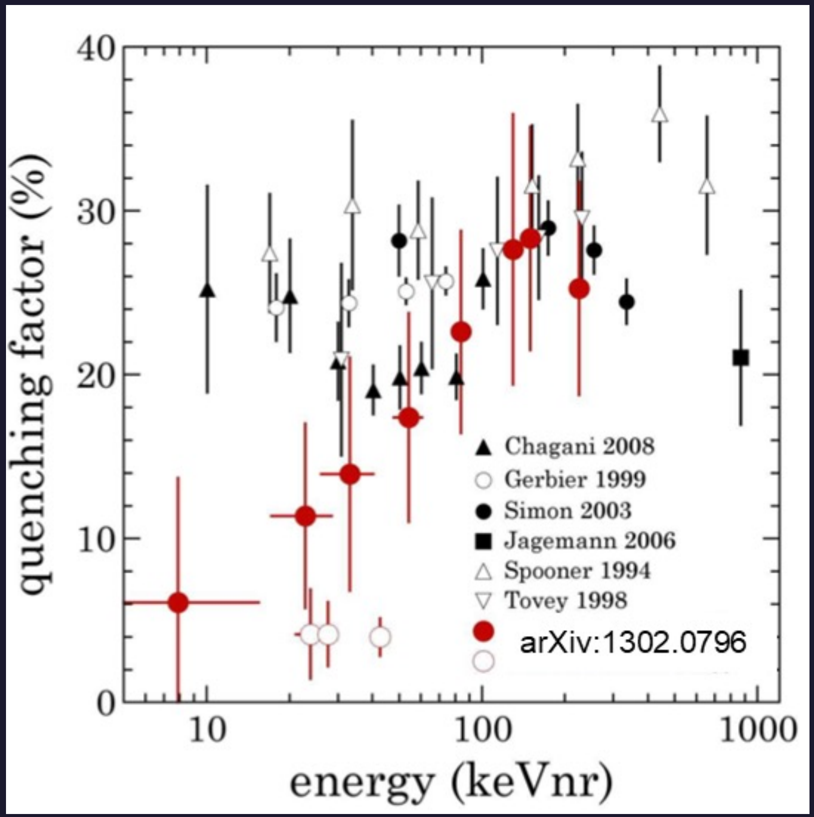

Example in case of DAMA	Na	I	Recoil energy range (keVee)	
Same method	0.30(1)	0.09(1)	6.5–97 (Na) 22–330 (I)	Phys. Lett. B389(1996)757
	0.4 ± 0.2	0.05 ± 0.02	5–100 (Na) 40–300 (I)	Phys. Rev. C47(1993)R425
semi-empirical formula	from 0.65 to 0.55	from 0.35 to 0.17	2–100	Astrop. Phys. 33(2010)40

Dark Matter investigation with crystal scintillators: «traditional approach»

KIMS-CsI(Tl): 12 crystals (104.4kg)

- Based on PSD between gamma and nuclear recoils
- Only statistical discrimination at low energy
- Limitation from systematics
- Uncertainties on exclusion plots

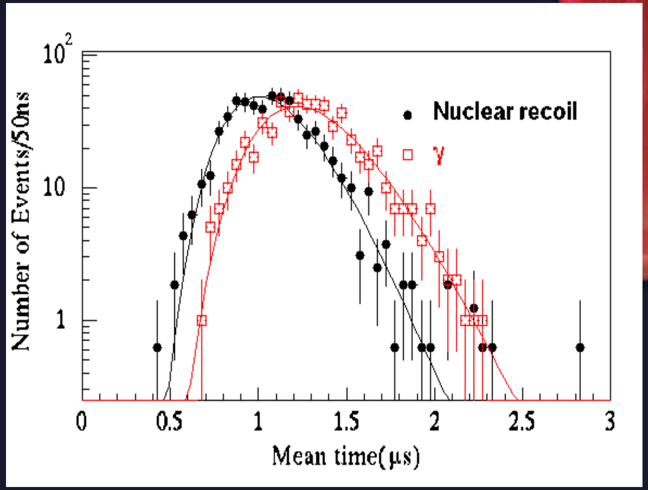

Dark Matter investigation with crystal scintillators: «traditional approach»

- Even very small systematics in the data selections and statistical discrimination and rejection procedures can be difficult to estimate;
- e.m. component of the rate can contain the signal or part of it
- Even assuming pure recoil case and ideal discrimination on an event-by-event base, the result will NOT be the identification of the presence of WIMP elastic scatterings as DM signal, because of the well-known existing recoil-like indistinguishable background;

Therefore, even in the ideal case the "excellent suppression of the e.m. component of the counting rate" can not provide a "signal identification"

→

A model independent signature is needed

Dark Matter investigation with crystal scintillators: signature

- Directionality: correlation of Dark Matter impinging direction with Earth's galactic motion due to the distribution of Dark Matter particles velocities $\Rightarrow$ very hard to realize

- Diurnal modulation: daily variation of the interaction rate due to different Earth depth crossed by the Dark Matter particles $\Rightarrow$ only for high σ

- Annual modulation: annual variation of the interaction rate due to Earth motion around the Sun at present the only feasible one, sensitive to many DM candidates and scenarios

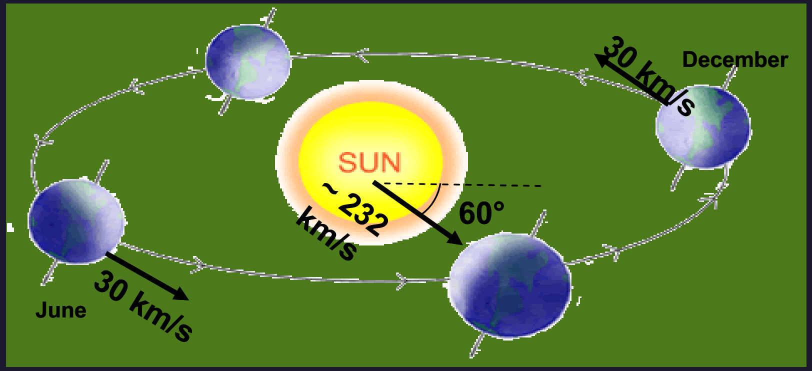

The annual modulation: a model independent signature for the investigation of DM particles

With the present technology, the annual modulation is the main model independent signature for the DM signal. Although the modulation effect is expected to be relatively small a suitable large-mass, low-radioactive set-up with an efficient control of the running conditions can point out its presence.

Drukier, Freese, Spergel PRD86; Freese et al. PRD88

Requirements

1) Modulated rate according cosine
2) In a definite low energy range
3) With a proper period (1 year)
4) With proper phase (about 2 June)
5) Just for single hit events in a multi-detector set-up
6) With modulation amplitude in the region of maximal sensitivity must be <7% for usually adopted halo distributions, but it can be larger in case of some possible scenarios

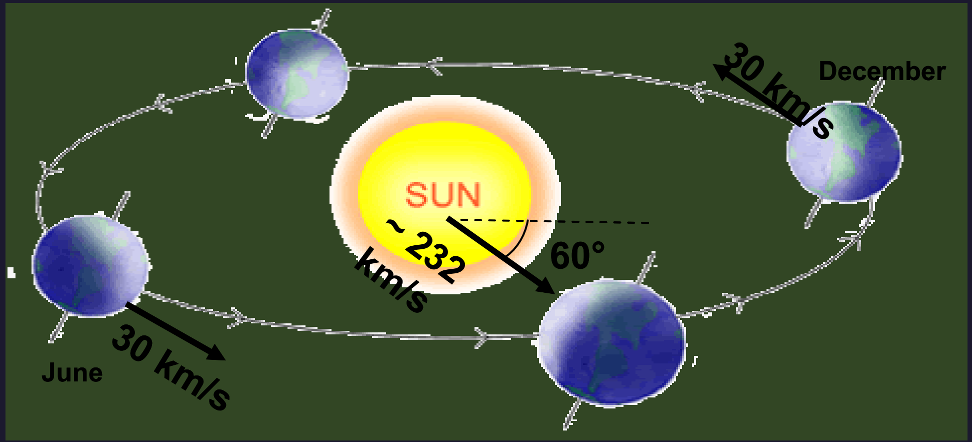

- v_{sun} ~ 232 km/s (Sun vel in the halo)
- v_{orb} = 30 km/s (Earth vel around the Sun)
- $\gamma = \pi/3$, $\omega = 2\pi/T$, T = 1 year
- t_0 = 2[nd] June (when $v_\oplus$ is maximum)

$$v_\oplus(t) = v_{sun} + v_{orb}\cos\gamma\cos[\omega(t-t_0)]$$

$$\boxed{S_k[\eta(t)] = \int_{\Delta E_k} \frac{dR}{dE_R} dE_R \cong S_{0,k} + S_{m,k}\cos[\omega(t-t_0)]}$$

the DM annual modulation signature has a different origin and peculiarities (e.g. the phase) than those effects correlated with the seasons

To mimic this signature, spurious effects and side reactions must not only be able to account for the whole observed modulation amplitude, but also to satisfy contemporaneously all the requirements

DAMA

DAMA experiment at LNGS

DAMA Collaboration has been developing and using low background crystal scintillators of different types to study rare processes

- DAMA/LIBRA (DAMA/NaI)
- DAMA/LXe
- DAMA/R&D
- DAMA/Crys
- DAMA/Ge

- Dark Matter investigation
- R&D for low background scintillators
- Results on several rare processes

see https://dama.web.roma2.infn.it/

Main results obtained by DAMA in the search for rare processes

- First or improved results in the search for 2β decays of ~30 candidate isotopes: ^{40}Ca, ^{46}Ca, ^{48}Ca, ^{64}Zn, ^{70}Zn, ^{100}Mo, ^{96}Ru, ^{104}Ru, ^{106}Cd, ^{108}Cd, ^{114}Cd, ^{116}Cd, ^{112}Sn, ^{124}Sn, ^{134}Xe, ^{136}Xe, ^{130}Ba, ^{136}Ce, ^{138}Ce, ^{142}Ce, ^{156}Dy, ^{158}Dy, ^{180}W, ^{186}W, ^{184}Os, ^{192}Os, ^{190}Pt and ^{198}Pt
- The best experimental sensitivities in the field for 2β decays with positron emission
- First observation of α decays of ^{151}Eu ($T_{1/2}$=5×10^{18}yr) with a CaF_2(Eu) scintillator and of ^{190}Pt to the first excited level (E_{exc}=137.2 keV) of ^{186}Os ($T_{1/2}$=3×10^{14}yr)
- Investigations of rare β decays of ^{113}Cd ($T_{1/2}$=8×10^{15}yr), ^{113m}Cd with $CdWO_4$ scintillator and ^{48}Ca with a CaF_2(Eu) detector
- Observation of correlated e^+e^- pairs emission in α decay of ^{241}Am ($A_{e+e-}/A_\alpha \approx 5\times10^{-9}$)
- CNC processes in ^{127}I, ^{136}Xe, ^{100}Mo and ^{139}La;
- Search for ^{7}Li solar axions using resonant absorption in LiF crystal
- Search for spontaneous transition of ^{23}Na and ^{127}I nuclei to superdense state;
- Search for cluster decays of ^{127}I, ^{138}La and ^{139}La;
- Search for PEP violating processes in sodium and in iodine;
- Search for N, NN, NNN decay into invisible channels in ^{129}Xe and ^{136}Xe

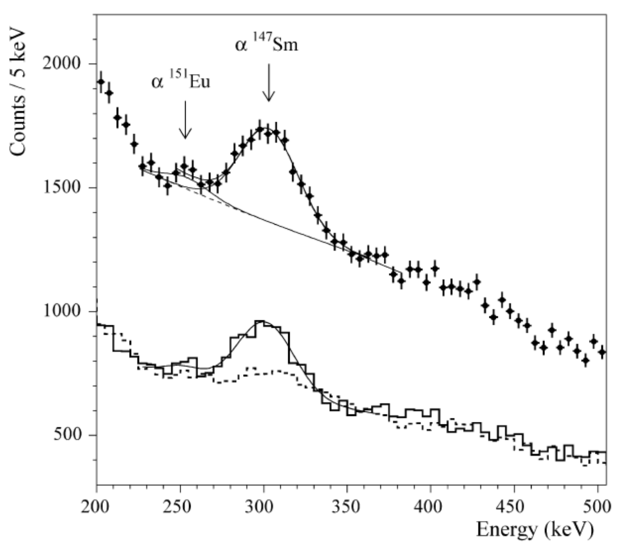

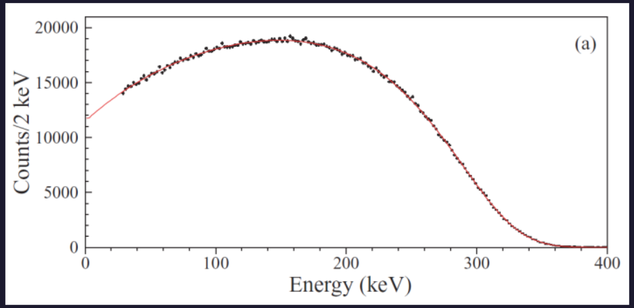

Many others are in progress

Highly radiopure NaI(Tl) experiment in DAMA

DAMA/NaI

Concluded on July 2002; 7 annual cycles, 0.29 ton×yr

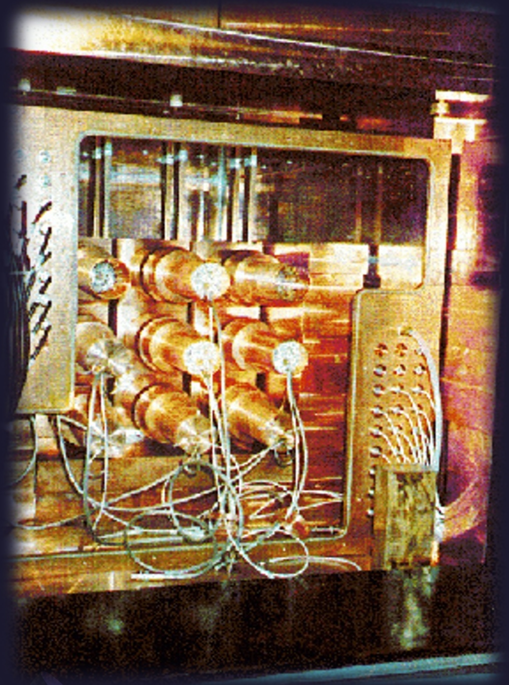

Model independent evidence of a particle DM component in the galactic halo at 6.3σ C.L.

+ many results on other rare processes

DAMA/LIBRA

New NaI(Tl) detectors with better radiopurity features; 3 phases of measurement with improved performances

Residual contaminations: ^{232}Th, ^{238}U and ^{40}K at level of 10^{-12} g/g

- DAMA/LIBRA-phase1: 7 annual cycles, 1.04 ton × yr
- Model independent evidence of a particle DM component in the galactic halo at 9.3σ C.L.
- DAMA/LIBRA-phase2: energy threshold 0.75-1 keV; 8 annual cycles released so far (1.53 ton × yr)

The pioneer DAMA/NaI: ≈100 kg highly radiopure NaI(Tl)

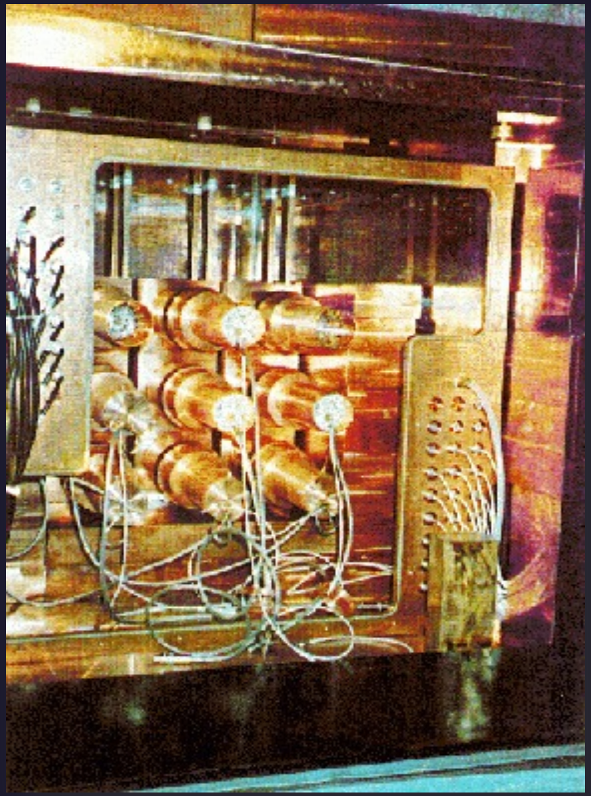

Completed in 2002, 7 annual cycles, total exposure **0.29 ton × yr**

Performances:

N.Cim.A112(1999)545-575, EPJC18(2000)283, Riv.N.Cim.26 n. 1(2003)1-73, IJMPD13(2004)2127

Results on rare processes:

- Possible Pauli exclusion principle violation — PLB408(1997)439
- CNC processes — PRC60(1999)065501
- Electron stability and non-paulian transitions in Iodine atoms (by L-shell) — PLB460(1999)235
- Search for solar axions — PLB515(2001)6
- Exotic Matter search — EPJdirect C14(2002)1
- Search for superdense nuclear matter — EPJA23(2005)7
- Search for heavy clusters decays — EPJA24(2005)51

Results on DM particles:

- PSD — PLB389(1996)757
- Investigation on diurnal effect — N.Cim.A112(1999)1541
- Exotic Dark Matter search — PRL83(1999)4918
- **Annual Modulation Signature** — PLB424(1998)195, PLB450(1999)448, PRD61(1999)023512, PLB480(2000)23, EPJC18(2000)283, PLB509(2001)197, EPJC23(2002)61, PRD66(2002)043503, Riv.N.Cim.26 n.1 (2003)1, IJMPD13(2004)2127, IJMPA21(2006)1445, EPJC47(2006)263, IJMPA22(2007)3155, EPJC53(2008)205, PRD77(2008)023506, MPLA23(2008)2125

Model independent evidence of a particle DM component in the galactic halo at 6.3σ C.L.

The DAMA/LIBRA set-up ~250 kg NaI(Tl) (Large sodium Iodide Bulk for RAre processes)

- Result of a 2nd generation R&D for more radiopure NaI(Tl) by exploiting new chemical/physical radiopurification techniques
- 25 x 9.7 kg NaI(Tl) in a 5x5 matrix + Suprasil-B light guides directly coupled to each bare crystal + 2 high Q.E. PMTs (40% at peak) for each crystal working in coincidence at the single ph. el. threshold
- Software energy threshold: 2 keV in phase1; 1 keV in phase2 (new PMTs, 6-10 phe/keV); 0.5 keV in phase2++
- Multiton-multicomponent passive shield (>10 cm of OFHC Cu, 15 cm of boliden Pb + Cd foils, 10/40 cm Polyethylene/paraffin, about 1 m concrete, mostly outside the installation)
- Three-level system to exclude Radon from the detectors
- Calibrations in the same running conditions as prod runs
- Fragmented set-up: single-hit events = each detector has all the others as anticoincidence
- Dismounting/Installing protocol in HPN_2
- All the materials selected for low radioactivity

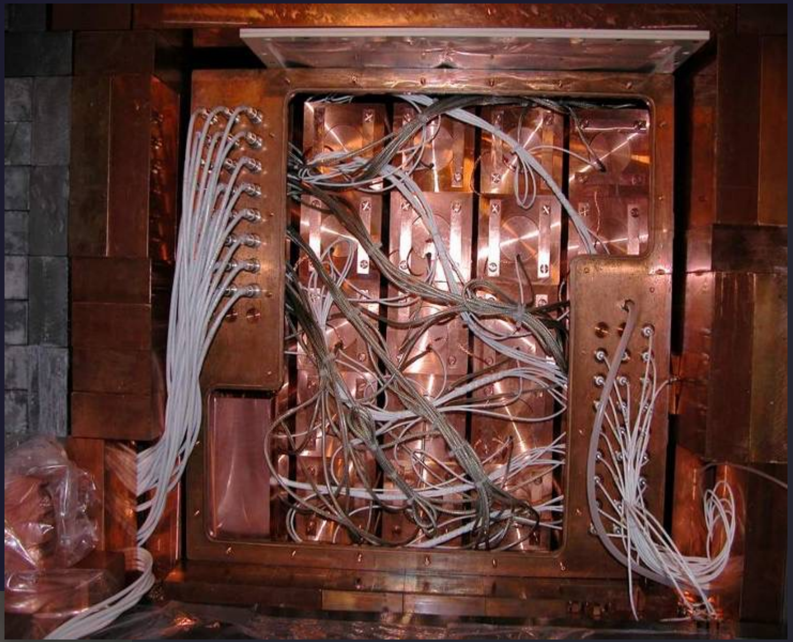

DAMA: model-independent Annual Modulation Result

experimental residuals of the single-hit scintillation events rate vs time and energy (in DAMA/LIBRA-phase2 1 keV thershold)

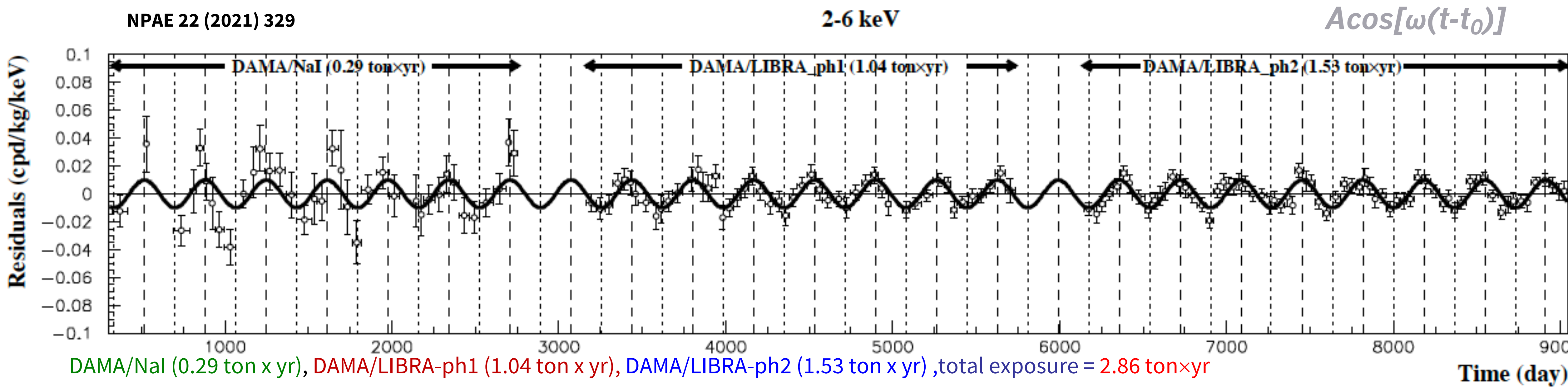

DAMA/NaI (0.29 ton x yr), DAMA/LIBRA-ph1 (1.04 ton x yr), DAMA/LIBRA-ph2 (1.53 ton x yr) ,total exposure = 2.86 ton×yr

- Absence of modulation? No

  $\chi 2/dof=311/156 \Rightarrow P(A=0)=2.3\times10^{-12}$
- *A=(0.00996 ±0.00074) cpd/kg/keV*

  $\chi 2/dof = 130/155$ *13.4 σ C.L.*

DAMA/NaI + DAMA/LIBRA-phase1 + phase2 favor the presence of a modulated behavior with proper features at 13.7 σ C.L.

Releasing period (T) and phase (t_0) in the fit

	ΔE	A(cpd/kg/keV)	$T=2\pi/\omega$ (yr)	t_0 (day)	C.L.
DAMA/LIBRA-ph2	(1-3) keV	0.0191±0.0020	0.99952±0.00080	149.6±5.9	9.6σ
	(1-6) keV	0.01058±0.00090	0.99882±0.00065	144.5±5.1	11.8σ
	(2-6) keV	0.00954±0.00076	0.99836±0.00075	141.1±5.9	12.6σ
DAMA/LIBRA-ph1 + DAMA/LIBRA-ph2	(2-6) keV	0.00959±0.00076	0.99835±0.00069	142.0±4.5	12.6σ
DAMA/NaI + DAMA/LIBRA-ph1 + DAMA/LIBRA-ph2	(2-6) keV	0.01014±0.00074	0.99834±0.00067	142.4±4.2	13.7σ

DAMA: model-independent Annual Modulation Result

NPAE 22 (2021) 329

- No Modulation above 6 keV
- No modulation in the whole energy spectrum: studying integral rate at higher energy, R_{90}

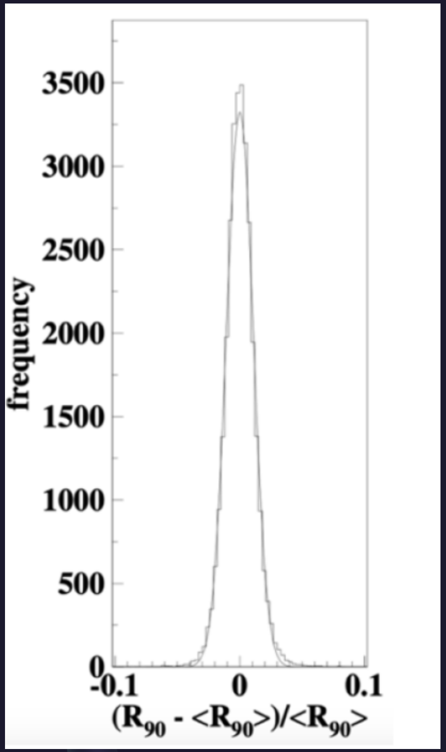

σ ≈ 1%, fully accounted by statistical considerations

- R_{90} percentage variations with respect to their mean values for single crystal in the DAMA/LIBRA running periods
- Fitting the behaviour with time, adding a term modulated with period and phase as expected for DM particles:

  ⇒ **consistent with zero**

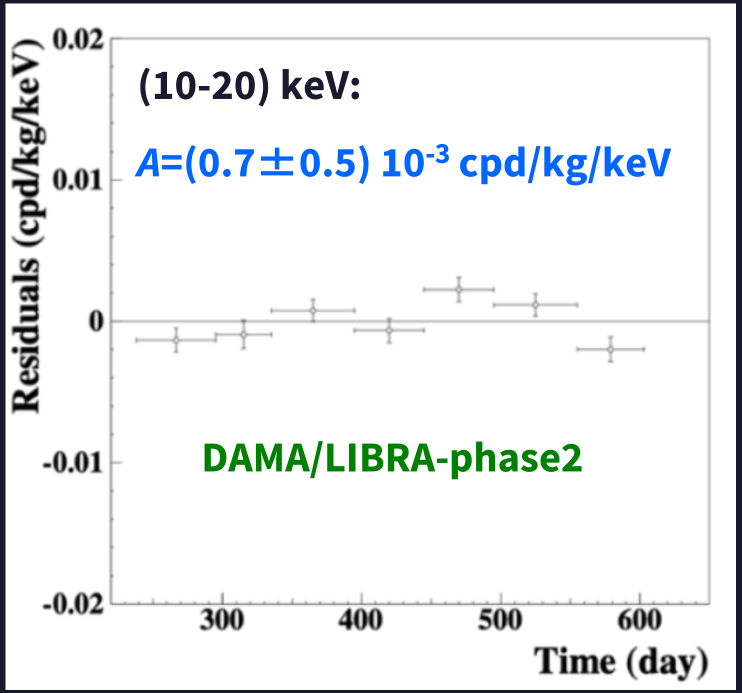

+ if a modulation present in the whole energy spectrum at the level found in the lowest energy region → R_{90} ~ tens cpd/kg → ~ 100 σ far away

DAMA: model-independent Annual Modulation Result

NPAE 22 (2021) 329

- Multiple hits events analysis: Dark Matter particle “beam” “switched off”

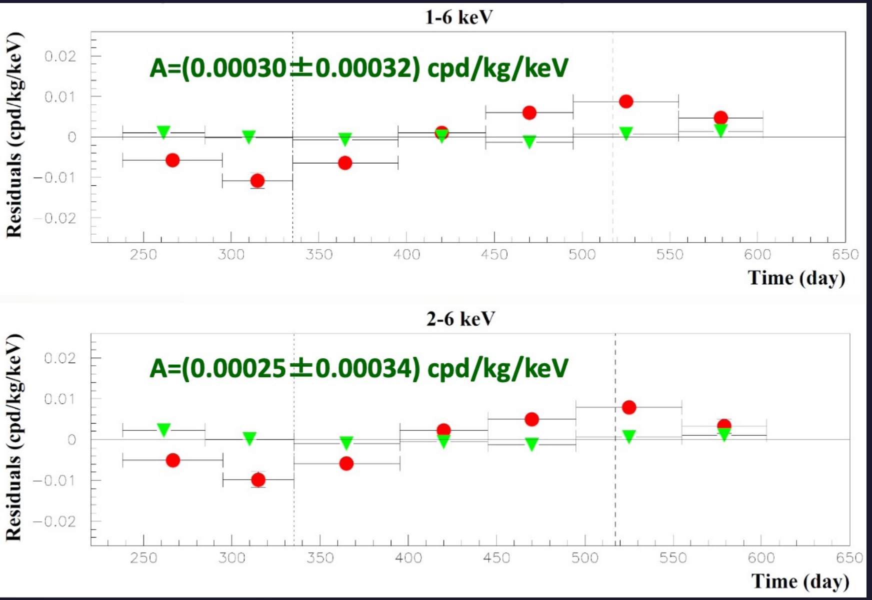

DAMA/LIBRA-phase2 (8 a.c., 1.53 ton × yr)

Single hit residual rate vs Multiple hit residual rate

- Clear modulation in the single hit events
- No modulation for multiple hit events

This result offers an additional strong support for the presence of DM particles in the galactic halo further excluding any side effect either from hardware or from software procedures or from background

- The analysis in frequency: DAMA/NaI + DAMA/LIBRA-(ph1+ph2) (22 yr), exposure: 2.86 ton × yr

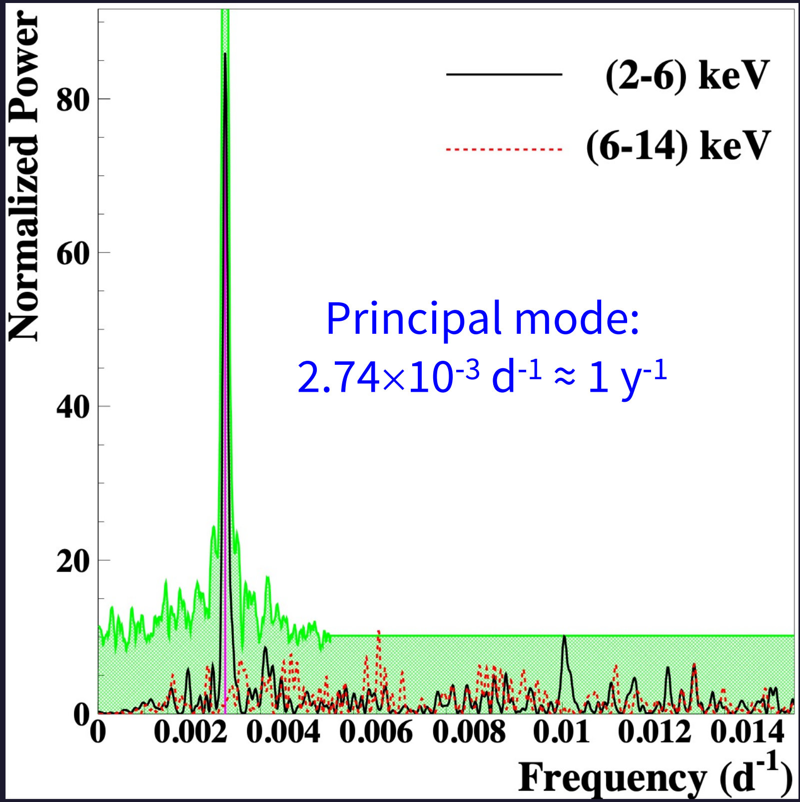

Zoom around 1 y^{-1} peak

Green area: 90% C.L. region calculated taking into account the signal in (2-6) keV

Clear annual modulation in (2-6) keV + only aliasing peaks far from signal region

DAMA: model-dependent analysis

A large (but not exhaustive) class of halo models and uncertainties are considered

NPAE 20(4) (2019) 317
PPNP114(2020)103810

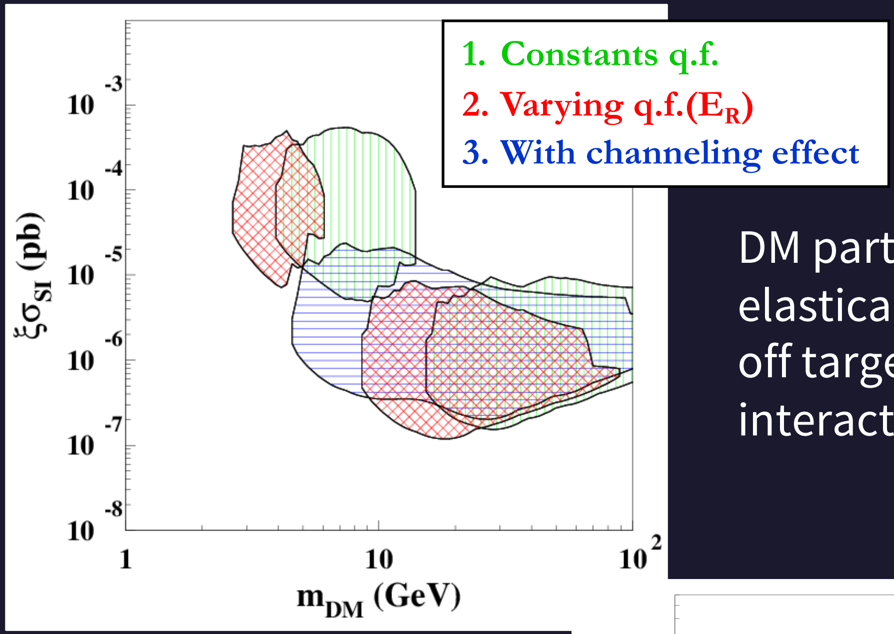

$$\sigma_{SI}(A,Z) \propto m_{red}^2(A,DM)\left[f_p Z + f_n(A-Z)\right]^2$$

Case of isospin violating SI coupling: $f_p \neq f_n$

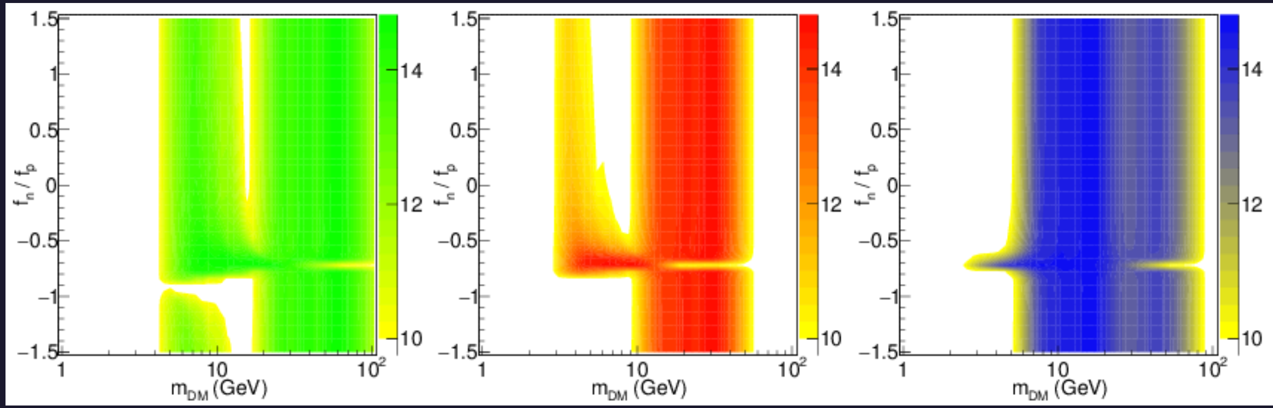

DM particles elastically scattering off target nuclei – SI interaction

- Two bands at low mass and at higher mass;
- Good fit for low mass DM candidates at $f_n/f_p \approx$ -53/74 = -0.72 (signal mostly due to ^{23}Na recoils).
- The inclusion of the uncertainties related to halo models, quenching factors, channeling effect, nuclear form factors, etc., can also support for f_n/f_p=1 low mass DM candidates either including or not the channeling effect.
- The case of isospin-conserving f_n/f_p=1 is well supported at different extent both at lower and larger mass.

Even a relatively small SD (SI) contribution can drastically change the allowed region in the (m_{DM}, $\xi\sigma_{SI(SD)}$) plane

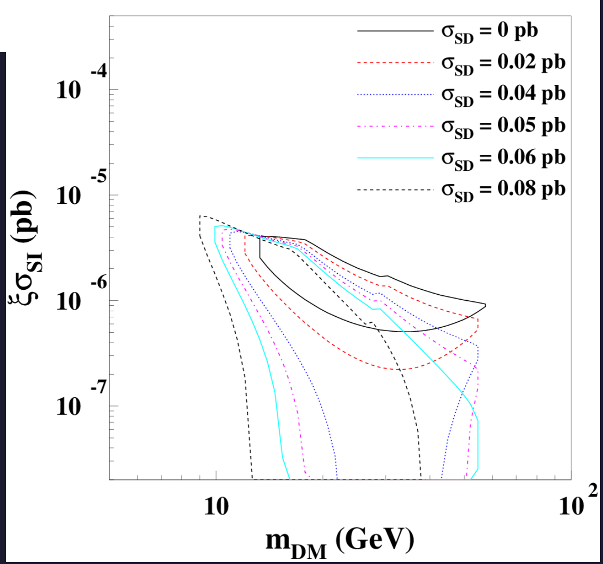

DAMA: model-independent Annual Modulation Result

NPAE 22 (2021) 329

- Max-likelihood analysis (T=1 yr , t_0= 152.5 day)
- DAMA/NaI + DAMA/LIBRA-phase1+ DAMA/LIBRA-phase2 (2.86 ton×yr)

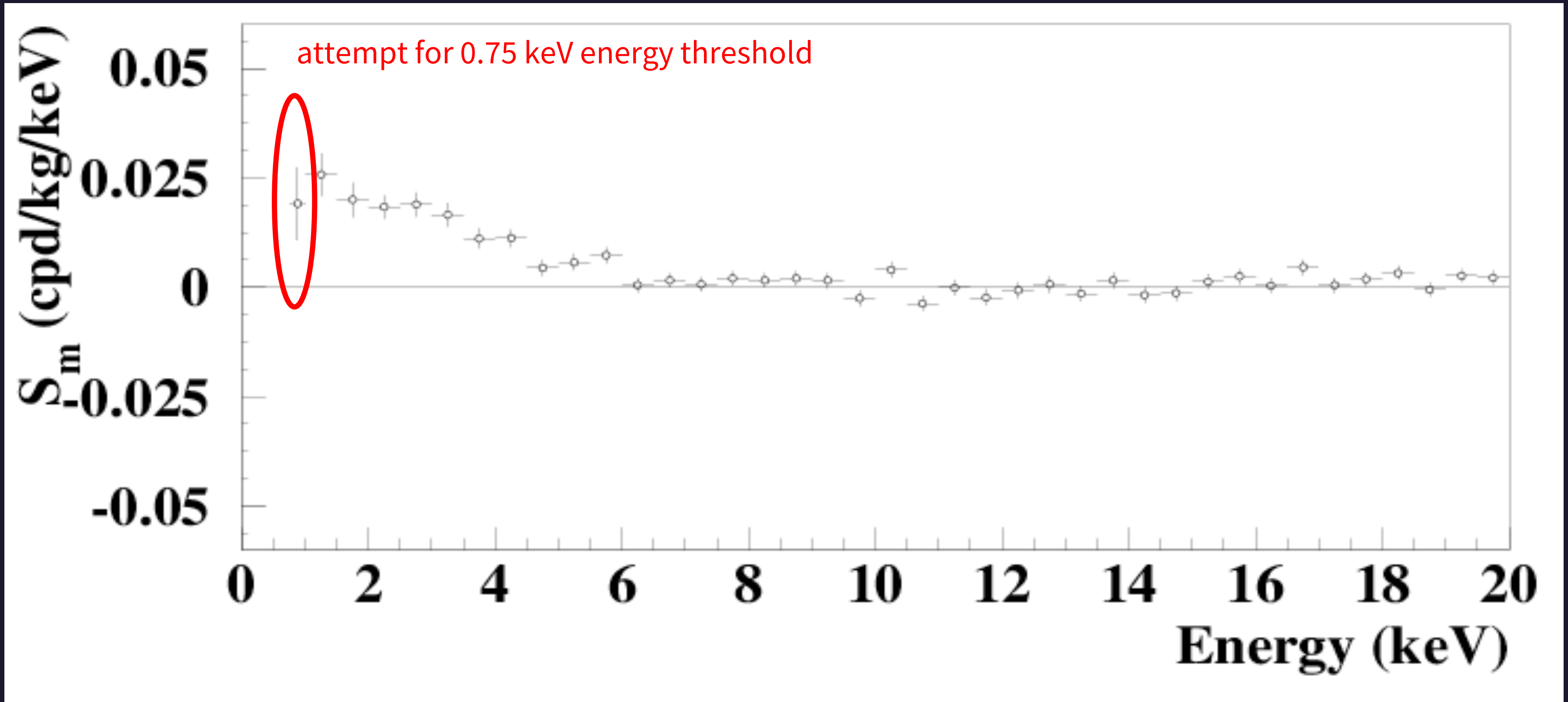

- A clear modulation is present in the (1-6) keV energy interval, while S_m values compatible with zero are present just above
- The S_m values in the (6–14) keV energy interval have random fluctuations around zero with χ^2 equal to 20.3 for 16 degrees of freedom (upper tail probability 21%).

Summary of possible systematics or side reactions in DAMA/LIBRA

Source	Main comment	Cautious upper limit (90%C.L.)
RADON	Sealed Cu box in HP Nitrogen atmosphere, 3-level of sealing, etc.	$<2.5\times10^{-6}$ cpd/kg/keV
TEMPERATURE	Installation is air conditioned+ detectors in Cu housings directly in contact with multi-ton shield$\rightarrow$ huge heat capacity + T continuously recorded	$<10^{-4}$ cpd/kg/keV
NOISE	Effective full noise rejection near threshold	$<10^{-4}$ cpd/kg/keV
ENERGY SCALE	Routine + intrinsic calibrations	$<1\text{-}2\times10^{-4}$ cpd/kg/keV
EFFICIENCIES	Regularly measured by dedicated calibrations	$<10^{-4}$ cpd/kg/keV
BACKGROUND	No modulation above 6 keV; no modulation in the (2-6) keV *multiple-hits* events; this limit includes all possible sources of background	$<10^{-4}$ cpd/kg/keV
SIDE REACTIONS	Muon flux variation measured at LNGS	$<3\times10^{-5}$ cpd/kg/keV

No systematics or side reaction able to mimic the exploited DM signature (i.e. to account for the whole measured modulation amplitude and to simultaneously satisfy all the requirements of the signature), has been found

COSINE

NaI(Tl) crystal scintillators for DM investigation: COSINE-100 experiment

- Collaboration between the DM-Ice and KIMS experiments
- Site: Yangyang underground laboratory in South Korea (700 m rock overburden)
- Detector: 8 NaI(Tl) crystals (106 kg) in liquid scintillator
- Experiment started to take physics data in September 2016 to study annual modulation as reported by DAMA

Crystal	Mass (kg)	Powder	Alpha rate (mBq/kg)	^{40}K (ppb)	^{238}U (ppt)	^{232}Th (ppt)	Light yield (p.e./keV)
Crystal 1	8.3	AS-B	3.20 ± 0.08	43.4 ± 13.7	< 0.02	1.31 ± 0.35	14.88 ± 1.49
Crystal 2	9.2	AS-C	2.06 ± 0.06	82.7 ± 12.7	< 0.12	< 0.63	14.61 ± 1.45
Crystal 3	9.2	AS-WS II	0.76 ± 0.02	41.1 ± 6.8	< 0.04	0.44 ± 0.19	15.50 ± 1.64
Crystal 4	18.0	AS-WS II	0.74 ± 0.02	39.5 ± 8.3		< 0.3	14.86 ± 1.50
Crystal 5	18.0	AS-C	2.06 ± 0.05	86.8 ± 10.8		2.35 ± 0.31	7.33 ± 0.70
Crystal 6	12.5	AS-WS III	1.52 ± 0.04	12.2 ± 4.5	< 0.018	0.56 ± 0.19	14.56 ± 1.45
Crystal 7	12.5	AS-WS III	1.54 ± 0.04	18.8 ± 5.3		< 0.6	13.97 ± 1.41
Crystal 8	18.3	AS-C	2.05 ± 0.05	56.15 ± 8.1		< 1.4	3.50 ± 0.33
DAMA			< 0.5	< 20	0.7 - 10	0.5 – 7.5	5.5 – 7.5

NaI(Tl) crystal scintillators for DM investigation: COSINE-100 experiment

Sci. Adv. 7, eabk2699 (2021)

- Last data released: Oct 2016-Jul 2018 (3 crystals not used), Exposure = 97.7 kg × year
- Traditional approach used by comparing experimental data with WIMP signal (model dependent analysis and result!)
- Experimental counting rate at keV higher than DAMA/LIBRA
- Not enough sensitivity to test DAMA/LIBRA

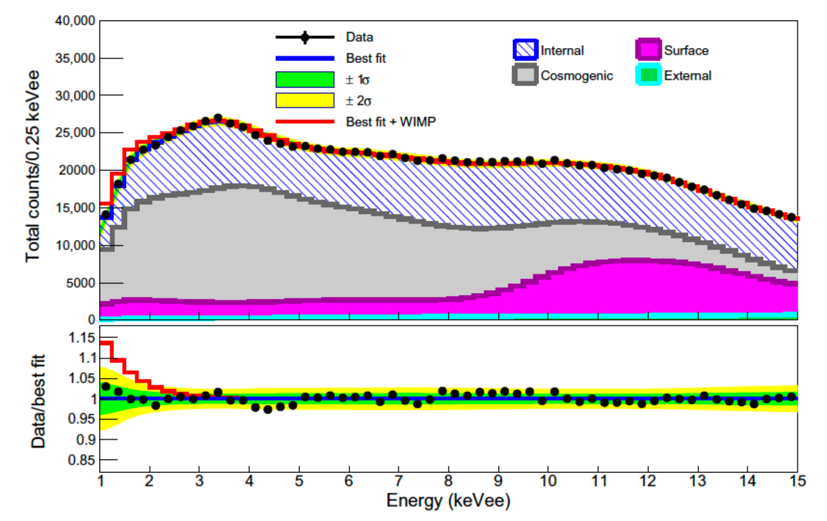

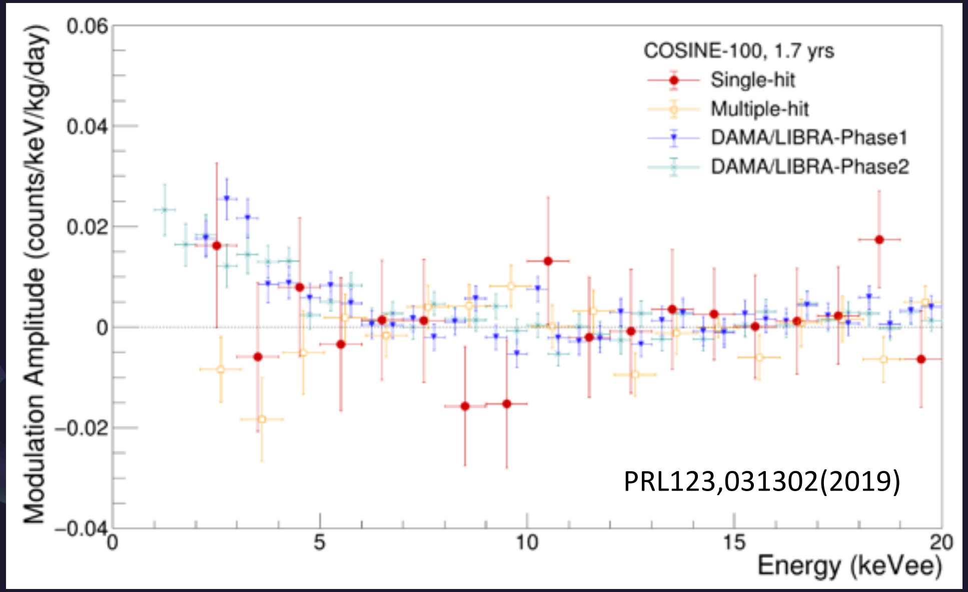

- Exclusion plots obtained are very sensitive to the models and parameters used in the calculation
- Different QF wrt DAMA crystals

NaI(Tl) crystal scintillators for DM investigation: COSINE-100 experiment

The methodology of the background subtraction (Cosine-100) is strongly discouraged and deprecated because of the impossibility to have a precise knowledge of the background contribution in particular at low energy, leading to large systematic uncertainties.

Very important discrepancies in the reconstruction of the structure at ≈ 45 keV, due to:

1. Missing contribute of ^{129}I (emended in a later paper, but not in the exclusion limits)
2. Overestimate contribute of ^{210}Pb

Cosine - Crystal #7

Components	Background 2-6 keV (dru)
Internal ^{210}Pb	1.50 +/- 0.07
Internal ^{40}K	0.05 +/- 0.01
Surface ^{210}Pb	0.38 +/- 0.21
^{3}H (Cosmogenic)	0.58 +/- 0.54
^{109}Cd (Cosmogenic)	0.09 +/- 0.09
Other cosmogenic	0.05 +/-0.03
External	0.03 +/- 0.02
Total expected	**2.70 +/- 0.59**
Data	**2.64 +/- 0.05**

Eur.Phys.J.C(2018)78 :490

[Unit: Counts/keV/kg/day]		Crystal 7
Data		2.492 ± 0.009
Total simulation		2.504 ± 0.210
Internal	^{210}Pb	0.999 ± 0.008
	^{40}K	0.046 ± 0.004
	Others	0.0048 ± 0.0001
Surface ^{210}Pb	Crystal	0.513 ± 0.131
	Teflon	0.051 ± 0.004
Cosmogenic	^{3}H	0.798 ± 0.164
	^{113}Sn	0.020 ± 0.002
	^{109}Cd	0.022 ± 0.002
	Others	0.015 ± 0.004
External ($\times 10^{-2}$)		3.374 ± 0.062

Eur.Phys.J.C(2021)81:837

Crystal #2, #3, #4, #6, #7
<data−model>$_{crystals}$ [1-6 keV] = −0.04±0.21 cpd/kg/keV
→ S_0[1-6 keV]<0.31 cpd/kg/keV 90%CL
Compatible with DAMA result

If the model of background is not correct the exclusion limits are meaningless

ANAIS

NaI(Tl) crystal scintillators for DM investigation: ANAIS experiment

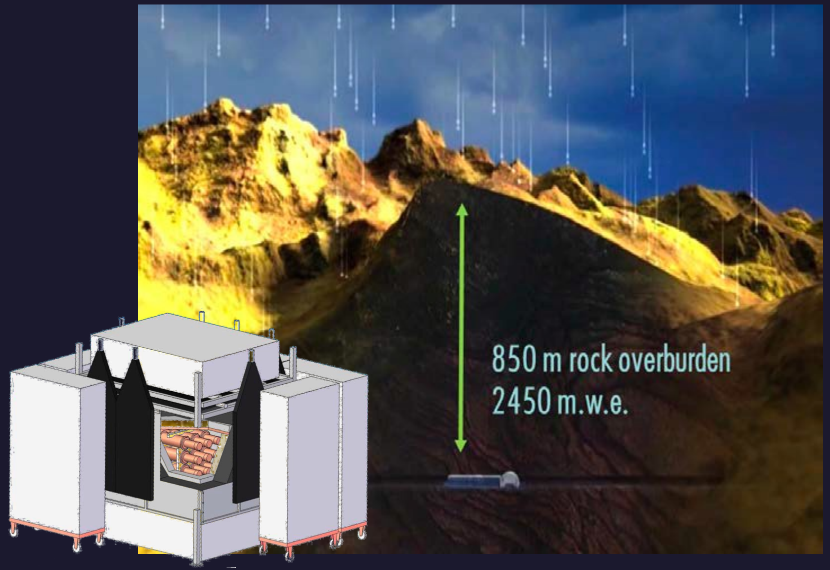

- Site: Canfranc Underground Laboratory, @ SPAIN (under 2450 m.w.e.)
- Detector: 9 NaI(Tl) crystals (112.5 kg) in a 3x3 matrix; light collection in all the nine modules ~ 15 p.e./keV (12.7-15.8 p.e./keV)
- In data taking data since August 2017 to study annual modulation as reported by DAMA

ANAIS-112 set-up:

- 10 cm archaeological lead
- 20 cm low activity lead
- Tight box preventing Radon entrance
- 16 plastic scintillators acting as muon veto system
- 40 cm polyethylene / water

NaI(Tl) crystal scintillators for DM investigation: ANAIS experiment

- Last data release: 3 years annual cycles, exposure 313.95 kg×y
- Time dependent background
- Data analysis to extract modulation signal in the time dependent rate: robust background model mandatory
- No annual modulation signal observed
- Claimed incompatibility with DAMA at 3.3 (2.6) σ, for a sensitivity of 2.5 (2.7) σ

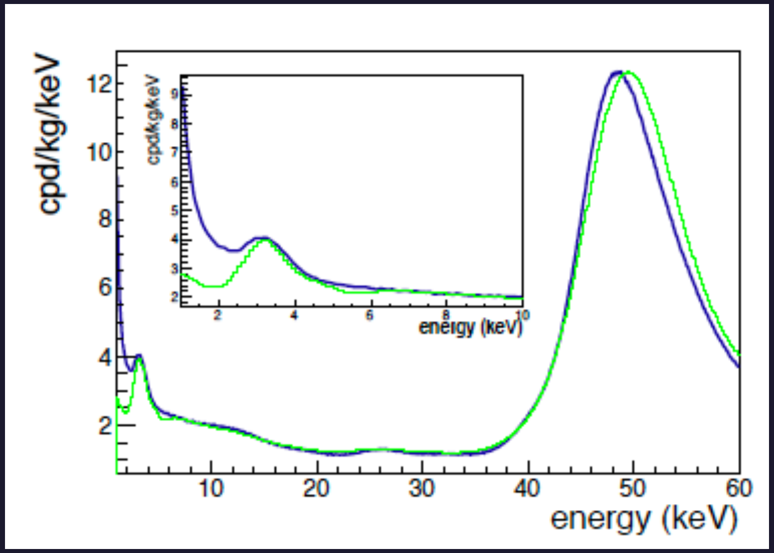

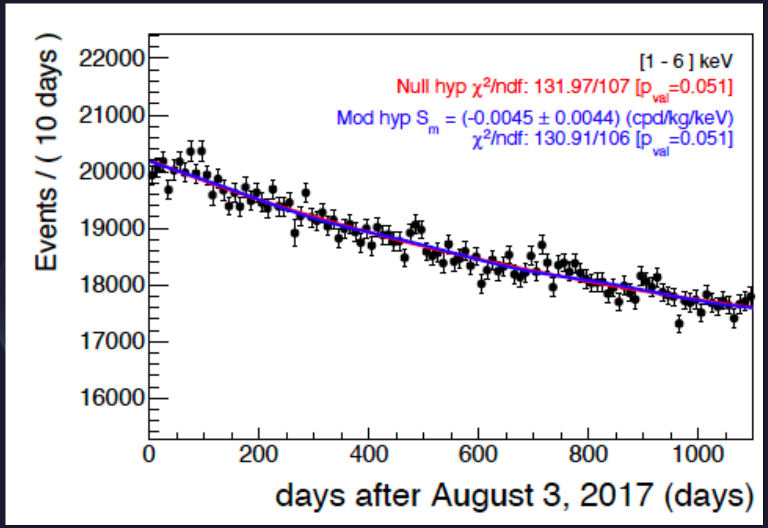

Modulation amplitudes from fit:
[1-6] keV: –0.0034±0.0042 cpd/kg/keV
[2-6] keV: 0.0003±0.0037 cpd/kg/keV)

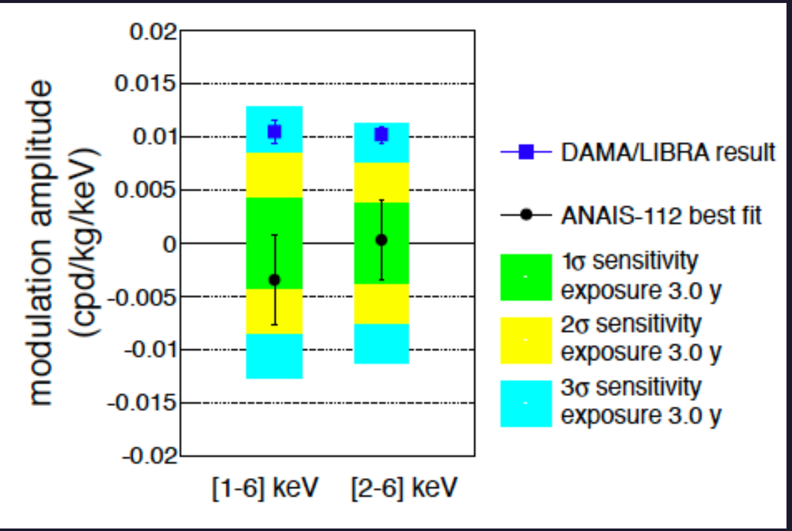

Phys. Rev. D 103, 102005 (2021)

About the results of ANAIS experiment

- ANAIS measures ≈ 5 times larger counting rate in [1,2] keV wrt DAMA/LIBRA-phase2
- High counting rate in ROI explained as populations, other than background, "*which could be leaking at the lowest energies in the ROI*" being the trigger rate "*dominated by other events, some of them with origin in the PMTs, others still unexplained*"
- In ANAIS the detection efficiencies of the applied cuts are **not** periodically evaluated with dedicated calibrations at very low energy as in DAMA/LIBRA
- The only check on stability of the cut-efficiencies is a fit on the counting rate of low energy events induced by the ^{22}Na or ^{40}K contaminations, selected in double coincidences, and with cuts applied

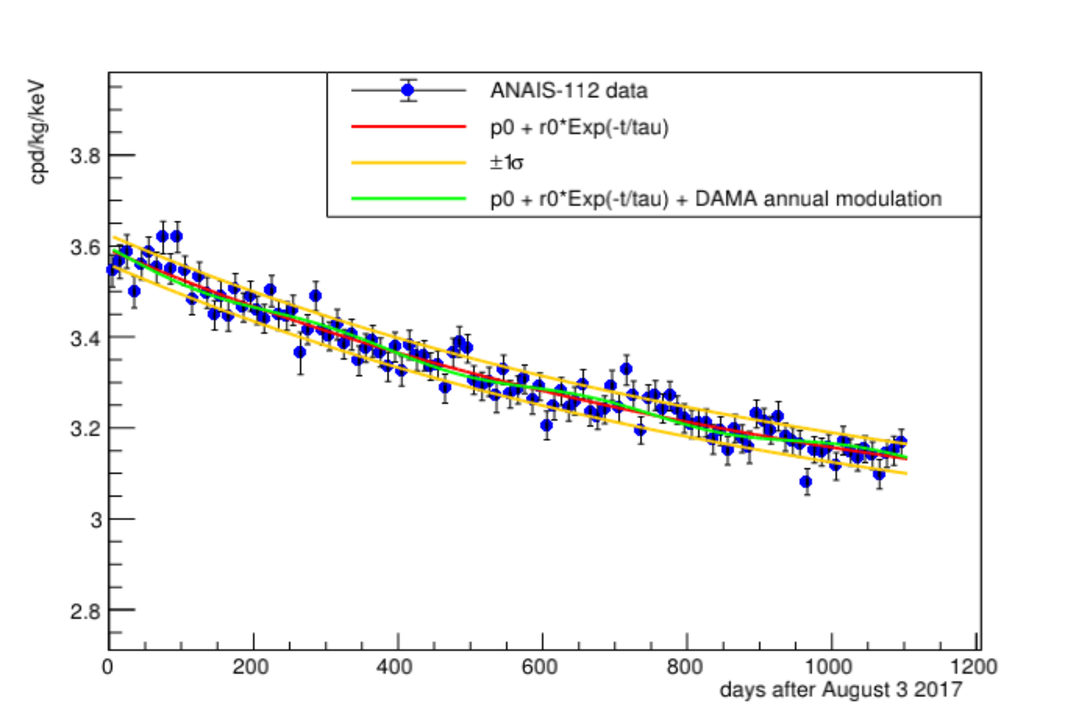

- Even **a 0.3% instability** of the ANAIS counting rate in the [1-6] keV region is enough to hide the annual modulation signal detected by DAMA: $A \approx 0.01$ cpd/kg/keV (green line in the plot)

About the nuclear quenching factor

- Different quenching factors are expected and measured for different NaI(Tl) crystals (they depends, e.g., on the used growing technique, on the different thallium doping concentration, …)
- A clear evidence is offered by the different α/β light ratio measured with DAMA and COSINE crystals
- As mentioned also in the ANAIS paper, this effect introduce a systematic uncertainty in the comparison with DAMA/LIBRA

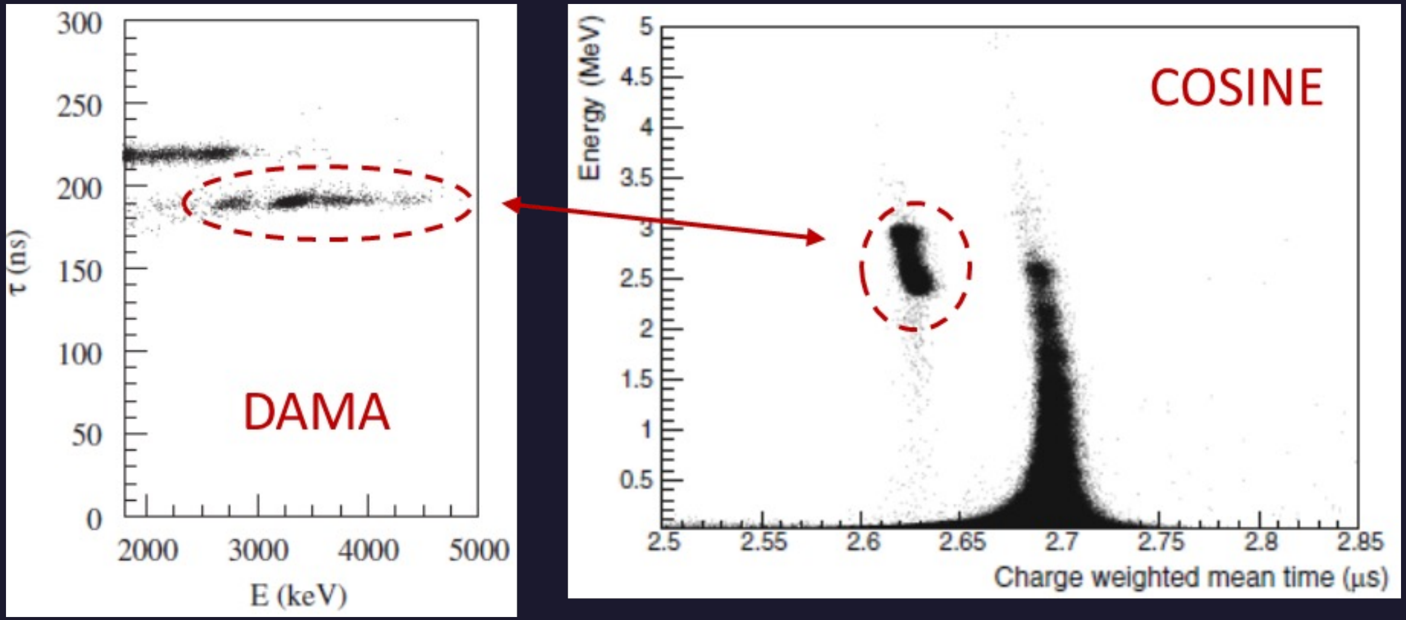

α events from ^{238}U and ^{232}Th chains in DAMA crystal span from 2.6 to 4.5 MeVee, while for the COSINE crystal they span from 2.3 to 3.0 MeVee

SABRE

SABRE: Sodium Iodide with Active Background REjection

from C. Tomei, SABRE Collaboration

Search for DM particles in the galactic halo through the annual modulation effect = signal from DM expected to modulate yearly with maximum in June.

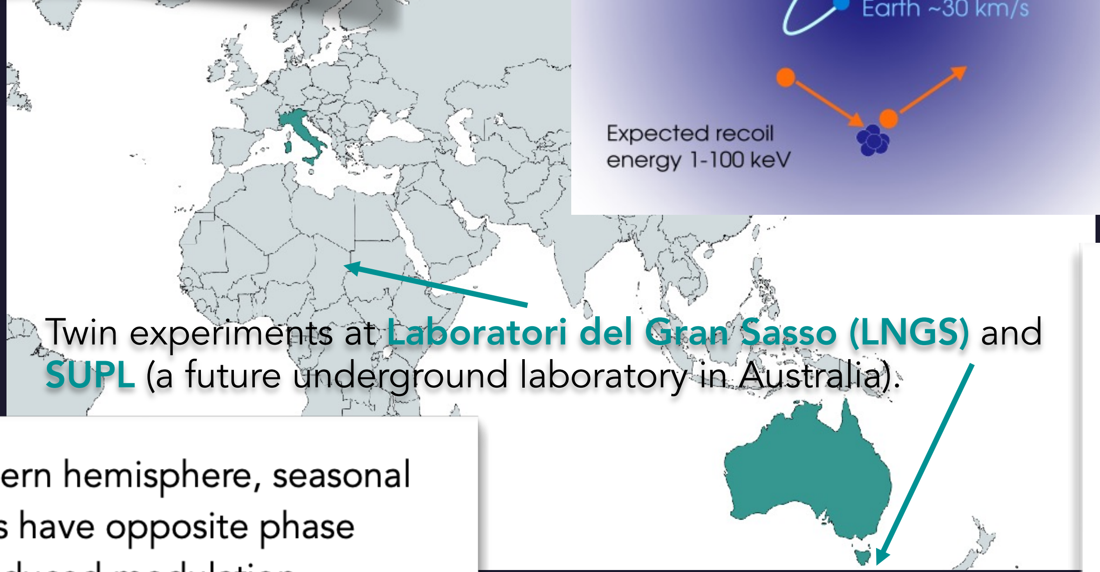

Twin experiments at **Laboratori del Gran Sasso (LNGS)** and **SUPL** (a future underground laboratory in Australia).

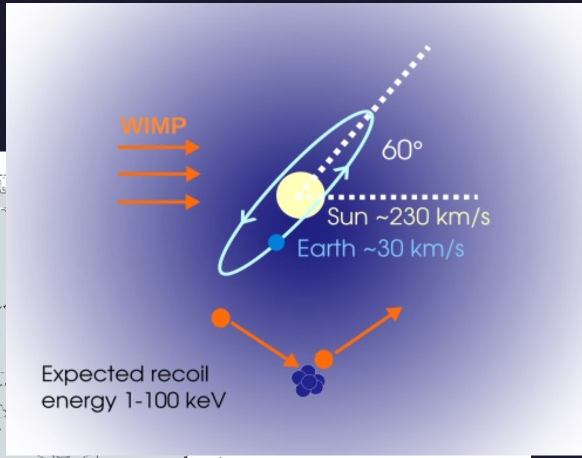

SABRE is a new experiment using NaI(Tl) scintillating crystals. Its goal is to reach an extremely low background.

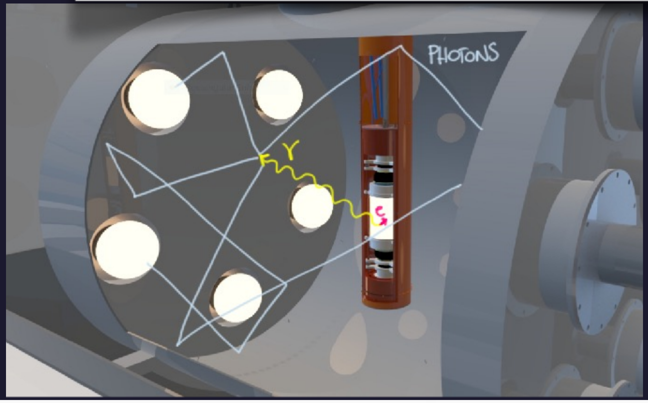

In the southern hemisphere, seasonal modulations have opposite phase while DM induced modulation maintains the same phase.

- NaI(Tl) scintillating crystal of ultra high radiopurity
- At SUPL, a **liquid scintillator veto** surrounding the NaI detectors at 4π, strongly reduces:
  - external backgrounds
  - internal backgrounds that release

SABRE PoP and SABRE-North full scale

A Proof of Principle (1 crystal+active veto) recently concluded @LNGS

Results:

- Breakthrough background level: ~1 count/day/kg/keV in the 1-6 keV ROI
- Active veto no longer required, need radiopure reflector

Goals for near future:

- Test the same crystal (NaI-33) with a new clean reflector
- Test reproducibility of crystal radiopurity
- Assembly of detector modules at LNGS with a new custom glovebox

→ Demonstrate feasibility of a full-scale experiment without active veto and finalize the design of crystal array + shielding

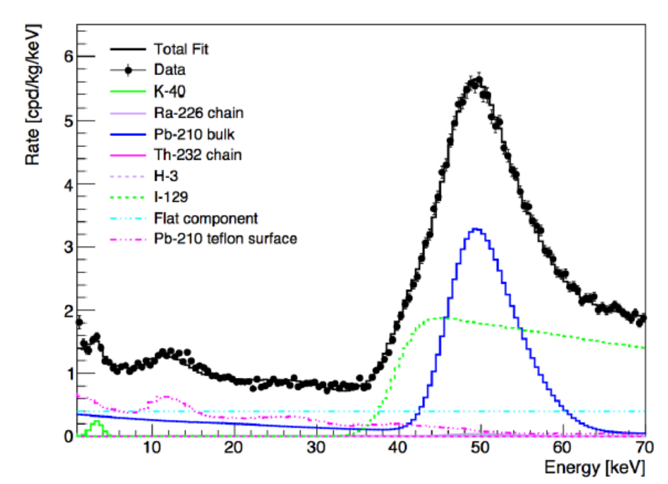

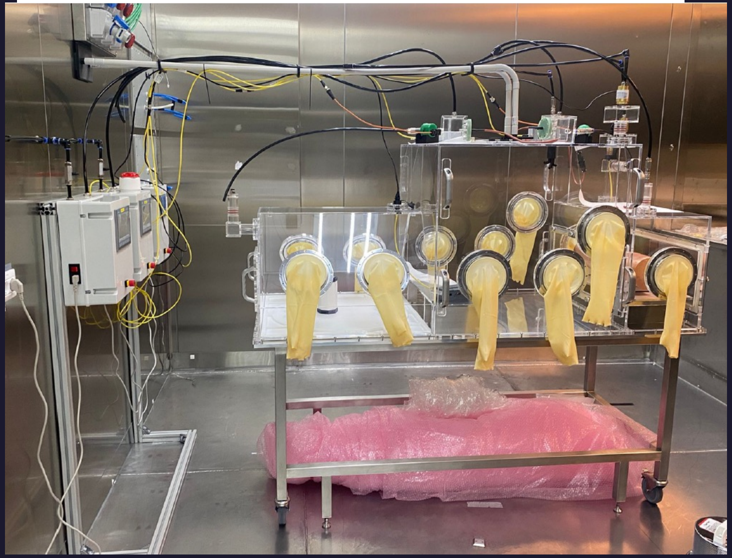

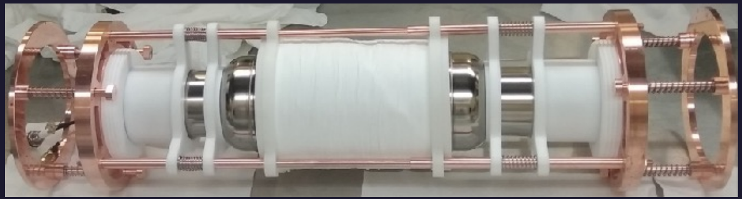

arXiv:2205.13876

$ZnWO_4$

Dark Matter with directionality approach

Based on the study of the correlation between the arrival direction of DM candidates able to induce a nuclear recoil and the Earth motion in the galactic frame

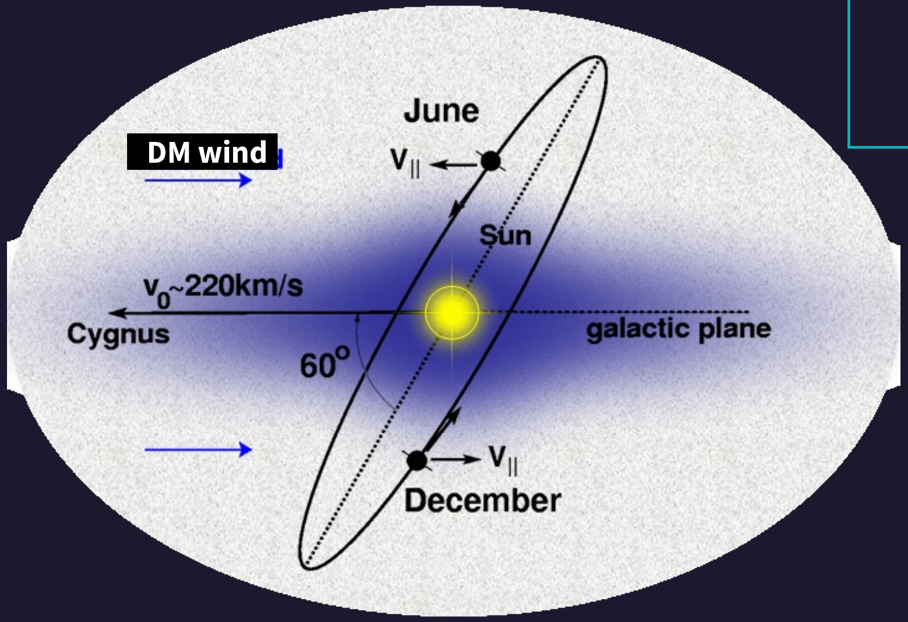

- Impinging direction of DM particle is (preferentially) opposite to the velocity of the Sun in the Galaxy

- Due to the Earth's rotation around its axis, the DM particles average direction with respect to an observer on the Earth changes with a period of a sidereal day

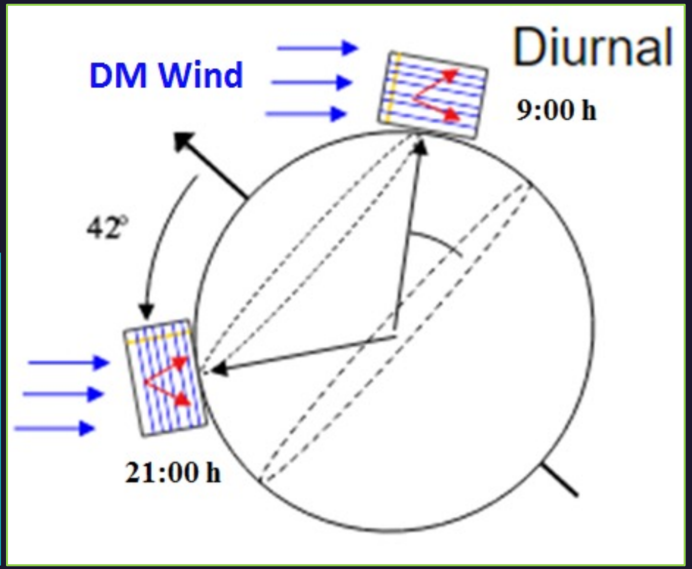

- The direction of the induced nuclear recoil is strongly correlated with that of the impinging DM particle
- The observation of an anisotropy in the distribution of nuclear recoil direction could give evidence for such DM candidates

A direction-sensitive detector is needed

Directionality with anisotropic scintillators

- Proposed for the first time in refs. [P. Belli et al., Il Nuovo Cim. C 15 (1992) 475], where the case of anthracene was analysed; some preliminary activities have been carried out [N.J.C. Spooner et al, IDM1997 Workshop; Y. Shimizu et al., NIMA496(2003)347]: the idea was revisited in [R. Bernabei et al., EPJC28(2003)203]

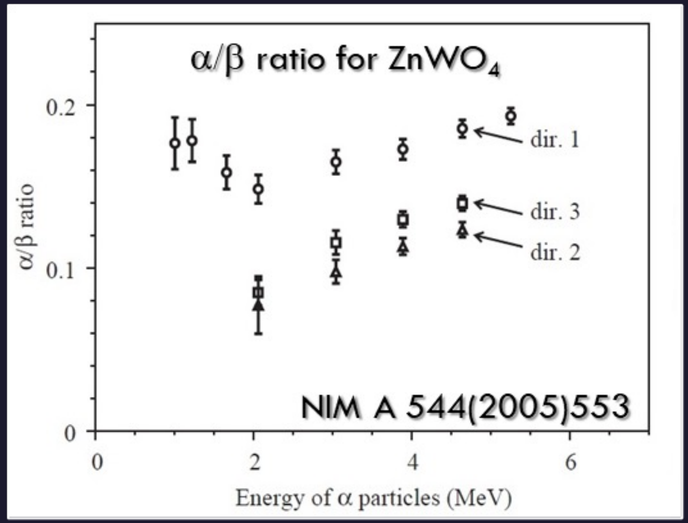

- Anisotropic Scintillator:
  - for heavy particles the light output and the pulse shape depends on the particle impinging direction with respect to the crystal axes
  - for γ/e the light output and the pulse shape are isotropic

- $ZnWO_4$ anisotropic scintillator: a very promising detector (NIMA544(2005)553, Eur. Phys. J. C 73 (2013) 2276, NIMA935(2019)89, Eur. Phys. J. A (2020) 56:83)
  1) very good anisotropic features;
  2) high level of radiopurity;
  3) high light output (improve at low temperature), that is low energy threshold feasible;
  4) high stability in the running conditions;
  5) sensitivity to small and large mass DM candidate particles;
  6) detectors with ~ kg masses

Signal rate in a given scenario

Eur. Phys. J. C 73 (2013) 2276

As a consequence of the light response anisotropy for heavy particles, recoil nuclei induced by the considered DM candidates could be discriminated from the background thanks to the expected variation of their low energy distribution along the day

The expected signal counting rate in the energy window (E1,E2) is a function of the time *t*
($v_d(t)$ the **detector velocity in the galactic rest frame**)

DM particle velocity in the laboratory frame

local DM halo density

number of target-nuclei (n) per mass unit

differential cross section in the c.m. frame

quenching factor, it depends on Ω_{out} the output direction of the nuclear recoil in the lab frame

recoiling nucleus kinetic energy in the laboratory frame

$$R(E_1,E_2,t)=\int d^3\vec{v}\int d\Omega_{cm}\,\frac{\rho_0 N_n}{m_{DM}}\left|\vec{v}\right| f[\vec{v}+\vec{v}_d(t)]\,\frac{d\sigma_n}{d\Omega_{cm}}\,\frac{1}{2}\left[erf\left(\frac{q_n(\Omega_{out})E_n-E_1}{\sqrt{2}\Delta}\right)-erf\left(\frac{q_n(\Omega_{out})E_n-E_2}{\sqrt{2}\Delta}\right)\right]$$

nuclear recoil direction in the center of mass frame

DM particle mass

DM velocity distribution in the galactic rest frame

detector energy resolution

NB: Many quantities are model dependent and a model framework has to be fixed: in this example, for simplicity, a set of assumptions and of values have been fixed, without considering the effect of the existing uncertainties on each one of them and without considering other possible alternatives

… the model framework considered here

- a simple spherical isothermal DM halo model with Maxwellian velocity distribution, 220 km/s local velocity, 0.3 GeV/cm^3 local density (ρ_0) and 650 km/s escape velocity;
- DM with dominant spin-independent coupling and the following scaling law (DM-nucleus elastic cross section, σ_n, in terms of the DM elastic cross section on a nucleon, σ_p):

$$\sigma_n = \sigma_p \left(\frac{M_n^{red}}{M_p^{red}} \cdot A \right)^2 = \sigma_p \left(\frac{m_p + m_{DM}}{m_n + m_{DM}} \cdot \frac{m_n}{m_p} \cdot A \right)^2$$

- a simple exponential form factor:

$$F_n^2(E_n) = e^{-\frac{E_n}{E_0}} \qquad E_0 = \frac{3(\hbar c)^2}{2 m_n r_o^2} \qquad r_0 = 0.3 + 0.91\sqrt[3]{m_n}$$

Quenching factor:

$$q_n(\Omega_{out}) = q_{n,x} \sin^2\gamma \cos^2\phi + q_{n,y} \sin^2\gamma \sin^2\phi + q_{n,z} \cos^2\gamma$$

where $q_{n,i}$ is the quenching factor value for a given nucleus, *n*, with respect to the *i*-th axis of the anisotropic crystal and $\Omega_{out} = (\gamma,\phi)$ is the output direction of the nuclear recoil in the laboratory frame

$q_{n,i}$ have been calculated following ref. [V.I. Tretyak, Astropart. Phys. 33 (2010) 40] considering the data of the anisotropy to α particles of the $ZnWO_4$ crystal

Energy resolution: $FWHM = 2.4\sqrt{E(keV)}$

Directionality: expected signal

- For an experiment performed at the LNGS latitude (**42°27′N**)
  - ⇒ at 21:00 h LST the DM particles come mainly from the top and
  - ⇒ 12 h later from the North and parallel to the horizon line

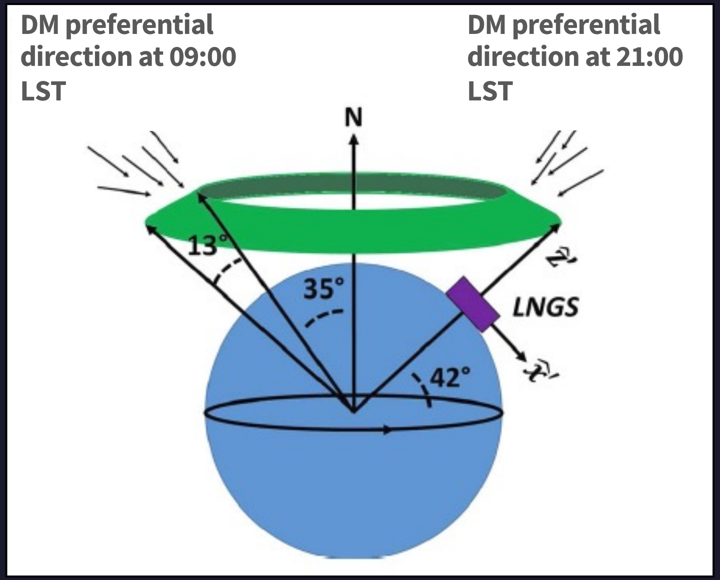

- Anisotropic detector response during a sidereal day is at maximum by arranging the $ZnWO_4$ crystal axis so that:
  - ➢ The one with the largest light output is vertical
  - ➢ The one with the smallest light output points north

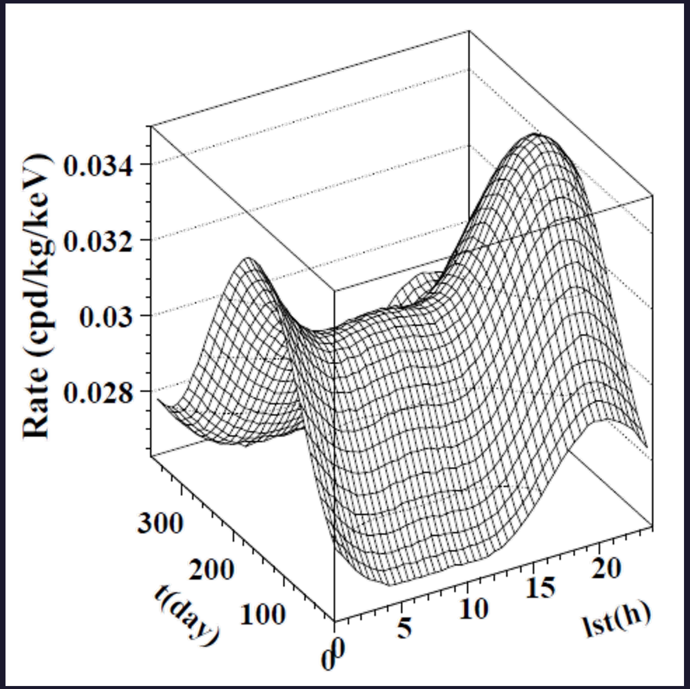

[2-3] keV
$\sigma_p = 5\times10^{-5}$ pb
$m_{DM} = 10$ GeV

- The diurnal effect refer to the sidereal day and not to the solar day
- Absolute maximum rate is at day 152 and at 21h LST (when the DM flux is at maximum and the DM preferential arrival direction is near the zenith)
- TEST:
  Identical sets of crystals placed in the same set-up with different axis orientation will observe consistently different time evolution of the rate

The signature is very distinctive and cannot be mimicked by background

ADAMO project: example of reachable sensitivity

Assumptions:

- simplified model framework (see before)
- 200 kg of $ZnWO_4$
- 5 years of data taking
- 2 keVee threshold
- four possible time independent background levels in the low energy region:
  - 10^{-4} cpd/kg/keV
  - 10^{-3} cpd/kg/keV
  - 10^{-2} cpd/kg/keV
  - 0.1 cpd/kg/keV

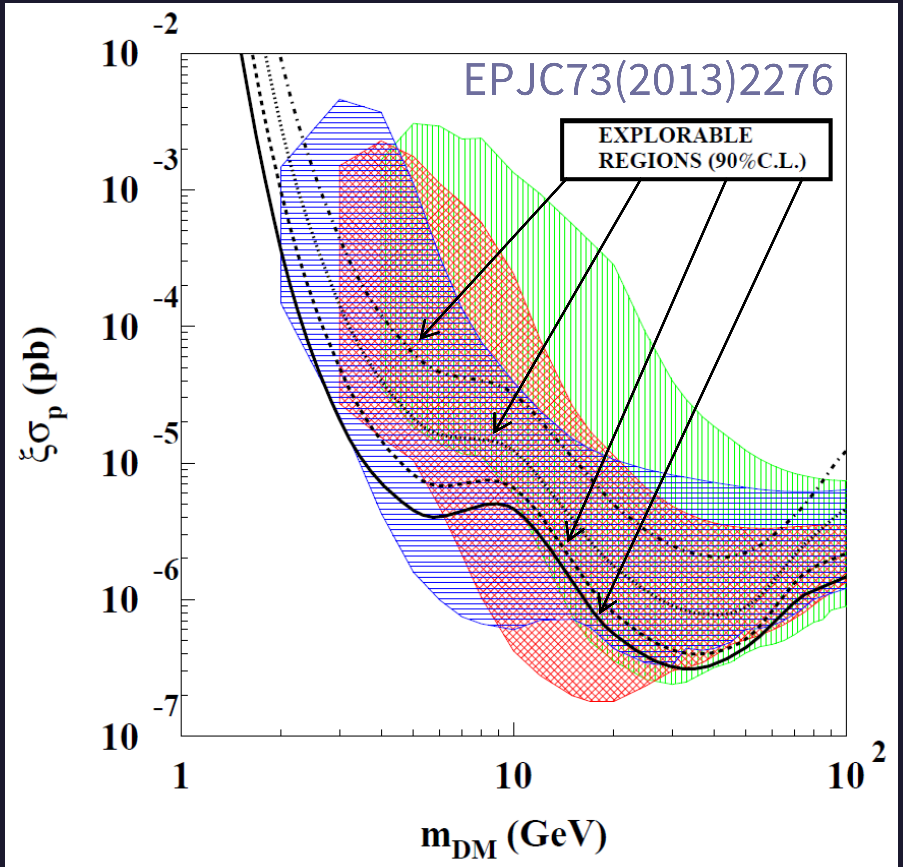

The directionality approach can reach in the given scenario a sensitivity to the cross section at level of 10^{-5} – 10^{-7} pb, depending on the particle mass

Allowed regions obtained with a corollary analysis of the 9.3σ C.L. DAMA model independent result in terms of scenarios for the DM candidates considered here (green, red and blue)

Response of the ZnWO4 to ^{241}Am α source

Eur.Phys.J.A 56 (2020) 83

- Calibration set-up:
  - PMT Hamamatsu H11934-200 (transit time ≈ 5 ns) + $ZnWO_4$
  - LeCroy Oscilloscope 24Xs-A, 2.5 Gs/s, 200MHz bandwidth
  - Pulse profiles acquired in a time window of 100 μs
- Crystal irradiated contemporaneously with γ (^{22}Na) and α (^{241}Am) sources along the three crystal axes
- Different α energies obtained with Mylar foils and measured with Si detector
- Very efficient PSD capability to discriminate α and γ

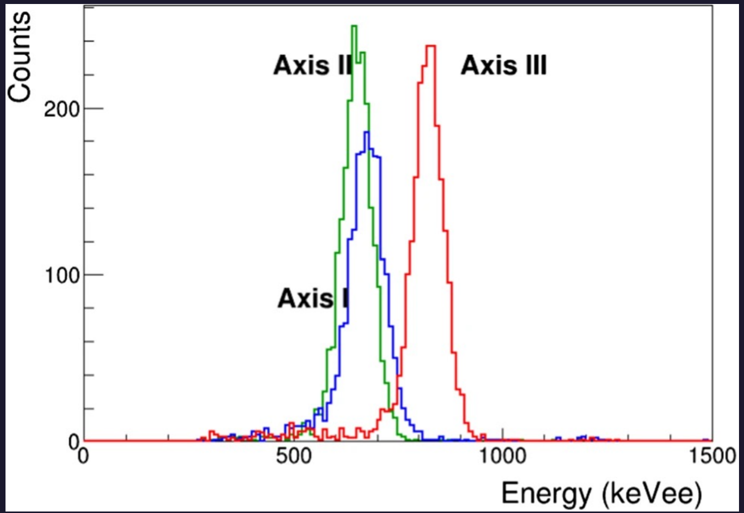

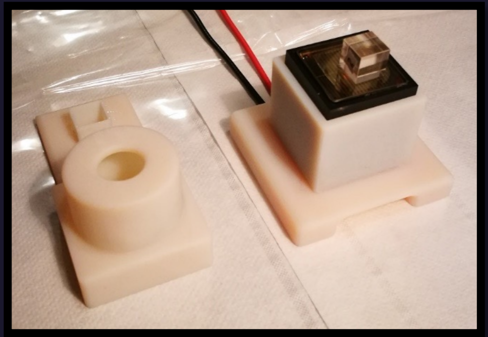

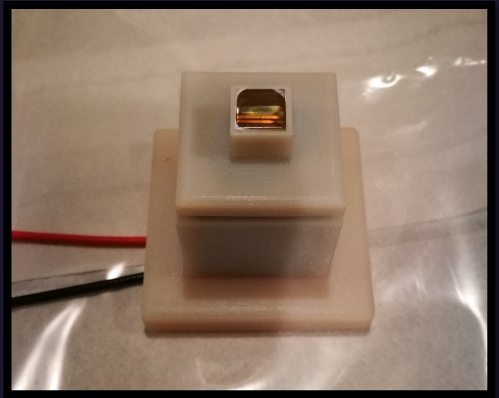

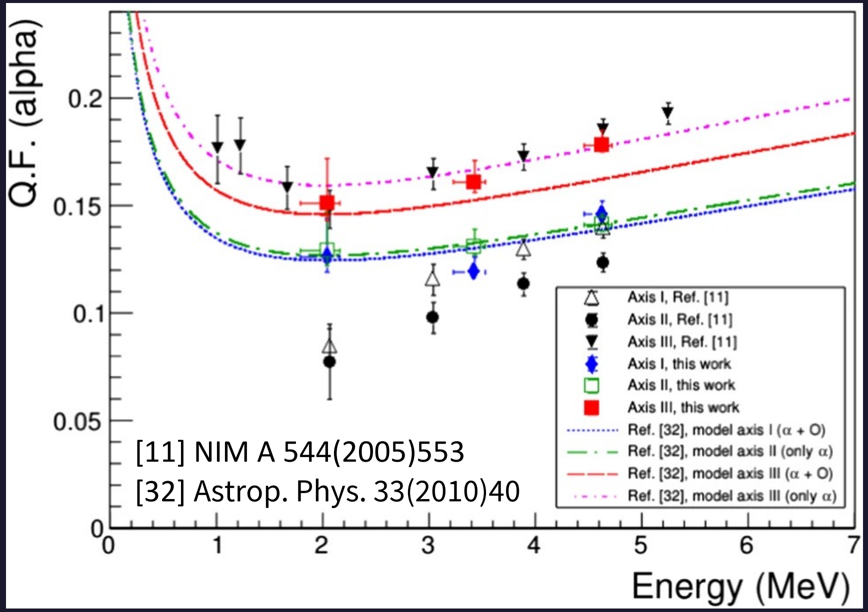

Response of the $ZnWO_4$ to monoenergetic neutrons

- Set-up:
  - ✓ $ZnWO_4$ Crystal (10 x 10 x 10 mm^3)
  - ✓ Two Hamamatsu PMTs: HAMA-H11934-200
  - ✓ 2 Neutron detectors (Scionix EJ-309)
  - ✓ Neutron Gun, Thermo Scientific MP320: 14 MeV neutrons

- Strategy: search for coincidence between a scattered neutron at a fixed angle and scintillation event in $ZnWO_4$ occurred in a well defined time window (TOF)
- Once fixed the θ angle, the recoil direction and energy are fixed
- Measurements performed at different θ angles and for different $ZnWO_4$ orientation (nuclear recoils along axes III and I)

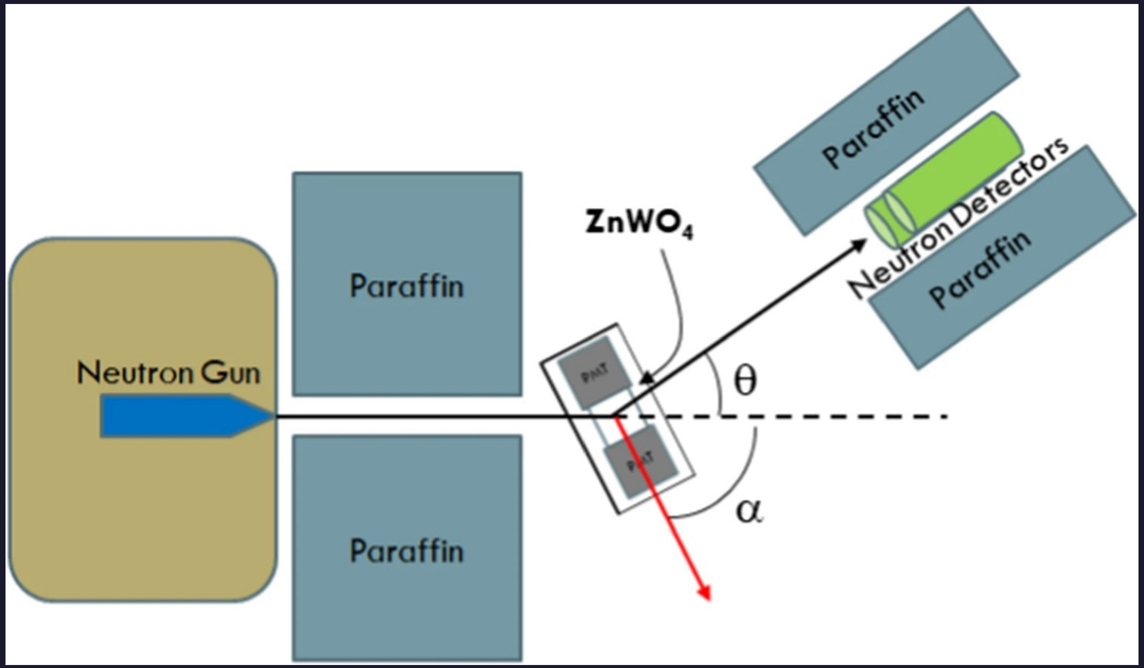

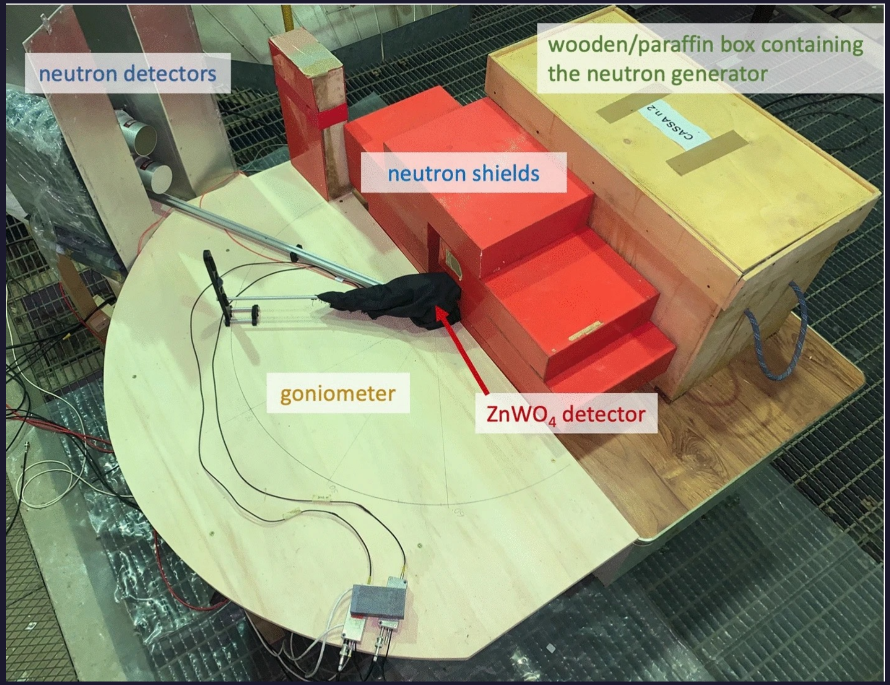

Eur.Phys.J.A 56 (2020) 83

Response of the $ZnWO_4$ to monoenergetic neutrons

Eur.Phys.J.A 56 (2020) 83

Energy distributions in $ZnWO_4$ for coincidence events when neutrons are identified in EJ-309 and two *TOF* windows are considered (case θ=80°):

- Events with proper *TOF* for **neutron induced recoils**
- Events with off-window *TOF:* **random coincidences**

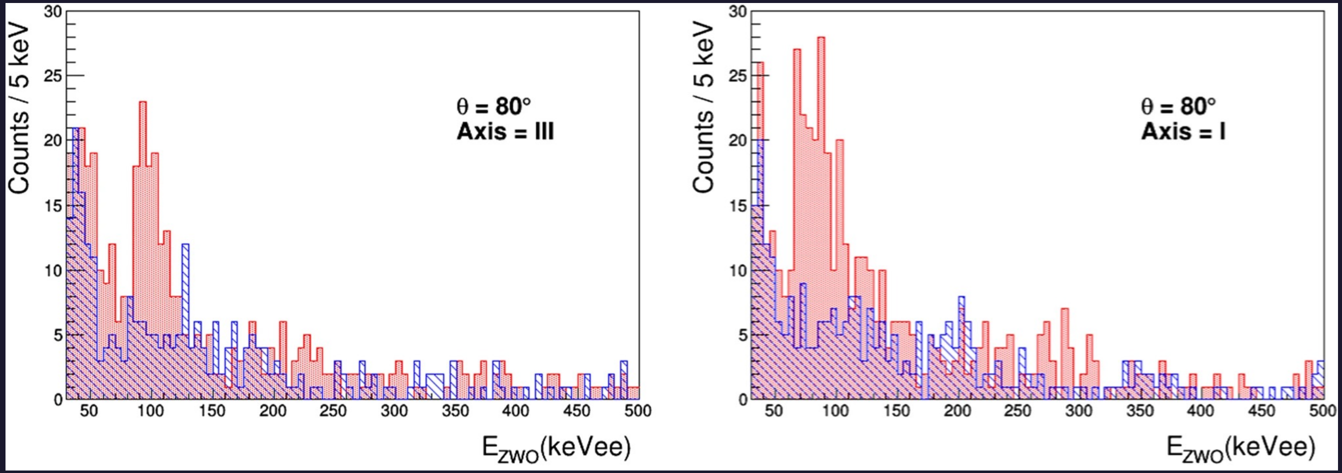

First evidence for anisotropy on the response of $ZnWO_4$ for nuclear recoils

θ	Crystal axis	E_{ZWO} (keVee)	σ (keVee)	$E_{R,O}$ (keV)	Quenching factor, Q	Q_{III}/Q_I
80°	III	99.3 ± 2.5	9	1402	0.0708 ± 0.0018	1.174 ± 0.051
	I	84.5 ± 2.9	12		0.0603 ± 0.0021	
70°	III	86.5 ± 2.0	7	1128	0.0767 ± 0.0018	1.121 ± 0.038
	I	77.2 ± 1.9	10		0.0684 ± 0.0017	
60°	III	75.4 ± 1.8	9	866	0.0871 ± 0.0021	1.166 ± 0.059
	I	64.7 ± 2.9	10		0.0747 ± 0.0033	

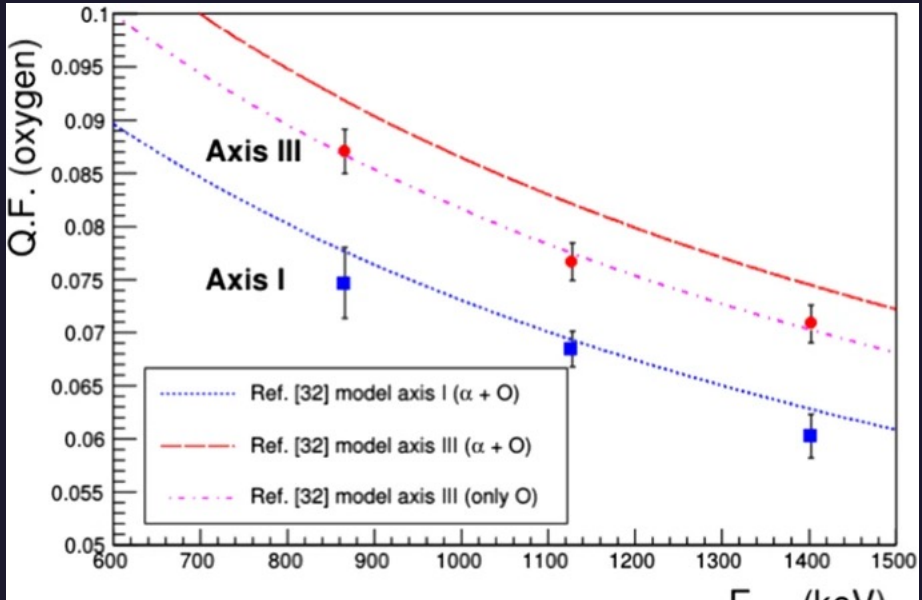

[32] Astrop. Phys. 33(2010)40

The anisotropy is significantly evident for oxygen nuclear recoils in the energy region down to hundreds keV at 5.4 σ confidence level

$SrI_2(Eu)$ crystal scintillator: a very promising detector for rare processes

Interesting scintillator for DM investigations and 2β ($2EC$, $EC\beta^+$) decay in ^{84}Sr:

- high light output <(≈100 000 photons/MeV)
- very high energy resolution (*FWHM* = 3% at 662 keV)
- possibility to grow crystals with large-size and uniform light yield
- radiopure (not natural long-lived radioactive isotopes)

Table 1
Properties of $SrI_2(Eu)$ crystal scintillators.

Property	Value
Density (g/cm^3)	4.5–4.6
Melting point (°C)	515
Structural type	Orthorhombic
Index of refraction	1.85
Wavelength of emission maximum (nm)	429–436
Light yield (photons/MeV)	$(68–120) \times 10^3$
Energy resolution (FWHM, %) for 662 keV γ of ^{137}Cs	2.6–3.7
Scintillation decay time (μs) under X-ray/γ ray excitation at 300 K	0.6–2.4

Radiopure Zr-based crystal scintillators: CZC

- Non hygroscopic crystal, LY ≈ 34800 photons/MeV, density = 3.36 g/cm^3
- Interesting new crystal scintillator to study:
  - $\beta\beta$ decay in ^{94,96}Zr and
  - rare single-β decay in ^{96}Zr
- The 2ν2β decay of ^{96}Zr already measured while single-β decay still not observed, $T_{1/2}^{expected}$=1.1×10^{20} yr (sixth-forbidden to gs and fourth-forbidden to the first two excited states of ^{96}Nb)
- Cs_2ZrCl_6 crystals scintillators developed in the framework of DAMA Collaboration
- Two Cs_2ZrCl_6 in data taking: expected sensitivity of 10^{21} yr for the 2β decay and $T_{1/2}$~1.4×10^{20} yr for the β decay of the ^{96}Zr

m=10.6(1)g
h =17.90(5) mm
Ø1=8.0(1) mm
Ø2=19.70(5) mm

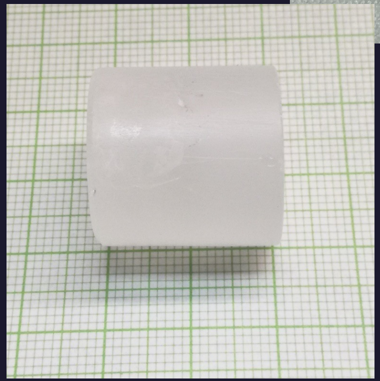

m=24.0(1)g
h =21.20(5) mm
Ø=21.00(5) mm

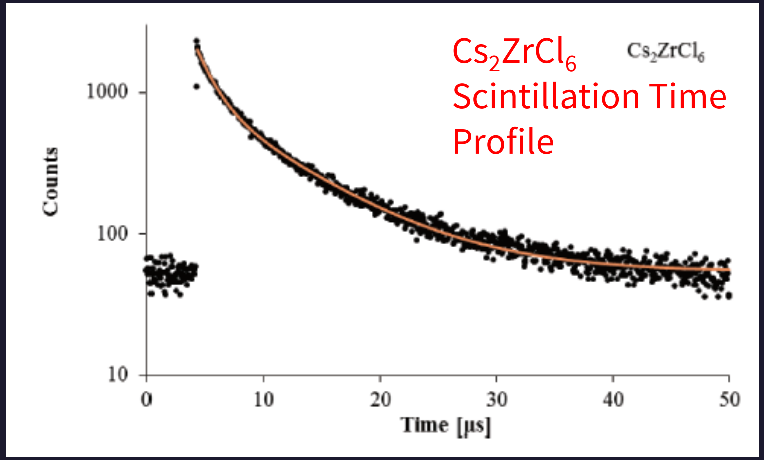

K. Saeki et al., Applied Physics Express 9, 042602 (2016)

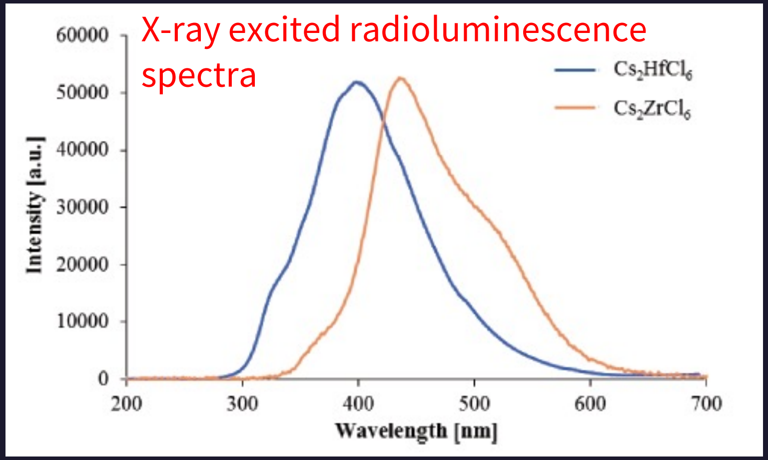

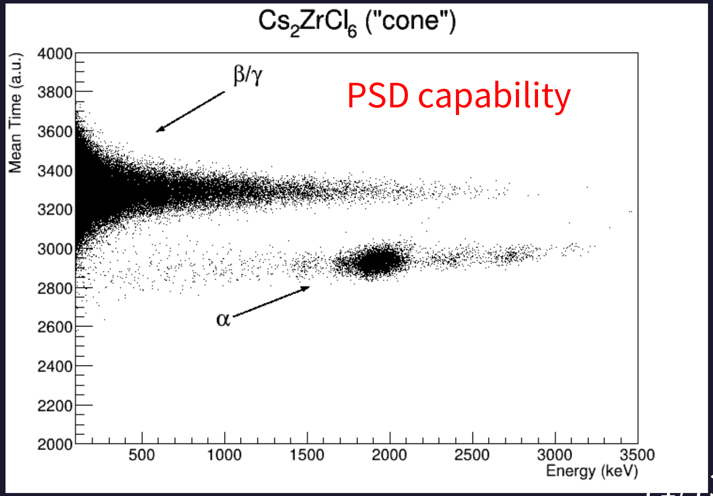

Radiopure Hf-based crystal scintillators: CHC

- Cs_2HfCl_6 crystal scintillator for studying the rare α and 2β decays of hafnium isotopes
- $LY \approx$ 50000 photons/MeV, $FWHM \approx$ 3.3% @ 662 keV, excellent PSD capability
- α decay candidates: ^{174}Hf, ^{176}Hf, ^{177}Hf, ^{178}Hf, ^{179}Hf, ^{180}Hf;
- 2β decay candidate: ^{174}Hf.

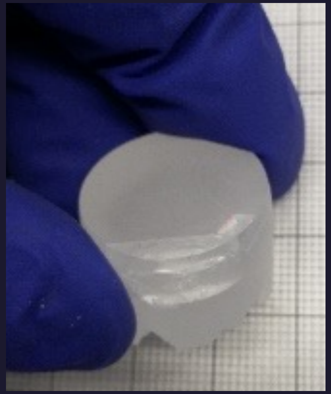

In the framework of DAMA Collaboration:

- A search for double beta decays in hafnium using HP-Ge gamma spectrometer
- Study of rare alpha decay in Hf isotopes using a crystal scintillators
- ^{174}Hf α decay to the ground state observed, **$T_{1/2}$ = 7.0(1.2) x 10^{16} y**
- $T_{1/2}$ limits of ^{176}Hf and ^{177}Hf α decay close to theoretical predictions

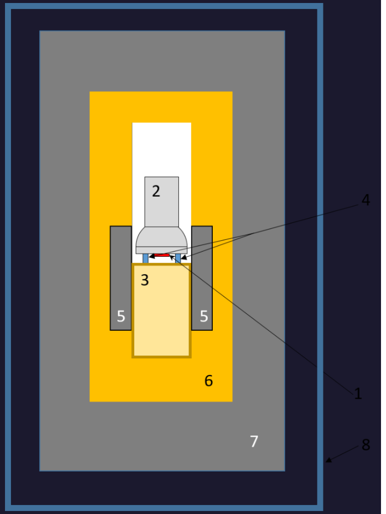

NPA 1002 (2020) 121941

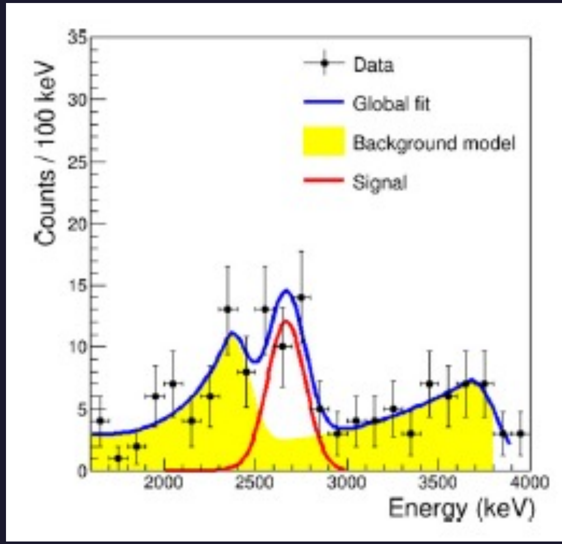

Measured spectrum in DAMA experiment

Conclusion

- Crystal scintillators at room temperature have been widely employed in underground physics and in Dark Matter investigation since the beginning of this field
- This technique has allowed to obtain important and competitive results by investigating many rare processes
- This technique can be further improved
- Annual modulation signal observed with ultra-radiopure NaI(Tl) by DAMA
- Crystal scintillators is still a valid approach for Dark Matter and offer also the possibility to study the directionality technique with anisotropic scintillators